

Satellite radar altimetry water elevations performance over a 200 m wide river: Evaluation over the Garonne River

Sylvain Biancamaria, Frédéric Frappart, A.-S Leleu, V. Marieu, D. Blumstein, Jean-Damien Desjonquères, F. Boy, A. Sottolichio, A. Valle-Levinson

▶ **To cite this version:**

Sylvain Biancamaria, Frédéric Frappart, A.-S Leleu, V. Marieu, D. Blumstein, et al.. Satellite radar altimetry water elevations performance over a 200 m wide river: Evaluation over the Garonne River. Advances in Space Research, 2017, 59 (1), pp.128-146. 10.1016/j.asr.2016.10.008 . hal-02136987

HAL Id: hal-02136987
https://hal.science/hal-02136987

Submitted on 22 May 2019

HAL is a multi-disciplinary open access archive for the deposit and dissemination of scientific research documents, whether they are published or not. The documents may come from teaching and research institutions in France or abroad, or from public or private research centers.

L'archive ouverte pluridisciplinaire **HAL**, est destinée au dépôt et à la diffusion de documents scientifiques de niveau recherche, publiés ou non, émanant des établissements d'enseignement et de recherche français ou étrangers, des laboratoires publics ou privés.

Satellite radar altimetry water elevations performance over a 200 m wide river: evaluation over the Garonne River

S. Biancamaria[1*], F. Frappart[1,2], A.-S. Leleu[1], V. Marieu[3], D. Blumstein[1,4], Jean-Damien Desjonquères[4], F. Boy[4], A. Sottolichio[3], A. Valle-Levinson[5]

[1] LEGOS, Université de Toulouse, CNES, CNRS, IRD, UPS - 14 avenue Edouard Belin, 31400 Toulouse, France

Email addresses: sylvain.biancamaria@legos.obs-mip.fr; anne-sophie.leleu@legos.obs-mip.fr; denis.blumstein@cnes.fr

[2] GET, Université de Toulouse, CNRS, IRD, UPS - 14 avenue Edouard Belin, 31400 Toulouse, France

Email address: Frederic.frappart@get.obs-mip.fr

[3] EPOC, Université de Bordeaux, CNRS - Bâtiment B18, allée Geoffroy Saint-Hilaire, CS 50023, 33615 Pessac Cedex, France

Email addresses: v.marieu@epoc.u-bordeaux1.fr; a.sottolichio@epoc.u-bordeaux1.fr

[4] CNES - 18 avenue Edouard Belin, 31401 Toulouse Cedex, France

Email addresses: jean-damien.desjonqueres@cnes.fr; francois.boy@cnes.fr

[5] University of Florida, Civil and Coastal Engineering Department, Gainesville, FL 32611, USA

Email address: arnoldo@ufl.edu

* Corresponding author – email sylvain.biancamaria@legos.obs-mip.fr - phone: +33561332915

Published in Advances in Space Research, doi:10.1016/j.asr.2016.10.008

Abstract

For at least 20 years, nadir altimetry satellite missions have been successfully used to first monitor the surface elevation of oceans and, shortly after, of large rivers and lakes . For the last 5-10 years, few studies have demonstrated the possibility to also observe smaller water bodies than previously thought feasible (river smaller than 500 m wide and lake below 10 km^2). The present study aims at quantifying the nadir altimetry performance over a medium river (200 m or lower wide) with a pluvio-nival regime in a temperate climate (the Garonne River, France). Three altimetry missions have been considered: ENVISAT (from 2002 to 2010), Jason-2 (from 2008 to 2014) and SARAL (from 2013 to 2014).

Compared to nearby in situ gages, ENVISAT and Jason-2 observations over the lower Garonne River mainstream (110 km upstream of the estuary) have the smallest errors, with water elevation anomalies root mean square errors (RMSE) around 50 cm and 20 cm, respectively. The few ENVISAT upstream measurements have RMSE ranging from 80 cm to 160 cm. Over the estuary, ENVISAT and SARAL water elevation anomalies RMSE are around 30 cm and 10 cm, respectively. The most recent altimetry mission, SARAL, does not provide river elevation measurements for most satellite overflights of the river mainstream. The altimeter remains “locked” on the top of surrounding hilly areas and does not observe the steep-sided river valley, which could be 50 m to 100 m lower. This phenomenon is also observed, for fewer dates, on Jason-2 and ENVISAT measurements. In these cases, the measurement is not “erroneous”, it just does not correspond to water elevation of the river that is covered by the satellite. ENVISAT is less prone to get ‘locked’ on the top of the topography due to some differences in the instrument measurement parameters, trading lower accuracy for more useful measurements. Such problems are specific to continental surfaces (or near the coasts), but are not observed over the open oceans, which are flatter.

To overcome this issue, an experimental instrument operating mode, called the DIODE/DEM tracking mode, has been developed by CNES (Centre National d’Etudes Spatiales) and has been tested during few Jason-2 cycles and during the first SARAL/AltiKA cycle. This

tracking mode “forces” the instrument to observe a target of interest, i.e. water bodies. The example of the Garonne River shows, for one SARAL ground track, the benefit of the DIODE/DEM tracking mode for a steep-sided river reach, which is not detected using the nominal instrument operating mode. Yet, this mode relies on ancillary datasets (a priori global DEM and global land/water mask), which are critical to obtain river valley observation. The ultimately computed elevations along the satellite tracks, loaded on board, should have an absolute vertical accuracy around 10 m (or better). This case also shows, when the instrument is correctly observing the river valley, that the altimeter can detect water bodies narrower than 100 m (like an artificial canal).

In agreement with recent studies, this work shows that altimeter missions can provide useful water elevation measurements over a 200 m wide river with RMSE as low as 50 cm and 20 cm, for ENVISAT and Jason-2 respectively. The seasonal cycle can be observed with the temporal sampling of these missions (35 days and 10 days, respectively), but short term events, like flood events, are most of the time not observed. It also illustrates that altimeter capability to observe a river is highly dependent of the surrounding topography, the observation configuration, previous measurements and the instrument design. Therefore, it is not possible to generalize at global scale the minimum river width that could be seen by altimeters.

This study analyzes, for the first time, the potential of the experimental DIODE/DEM tracking mode to observe steep-sided narrow river valleys, which are frequently missed with nominal tracking mode. For such case, using the DIODE/DEM mode could provide water elevation measurements, as long as the on board DEM is accurate enough. This mode should provide many more valid measurements over steep-sided rivers than currently observed.

Keywords: satellite altimetry; Garonne River; DIODE/DEM mode; ENVISAT; Jason-2; SARAL

1. Introduction

Continental waters play a key role in the Earth water cycle and are subject to complex interactions at the interface between the atmosphere and ocean. These waters directly impact human societies through food consumption, agriculture, and industrial activities. Continental waters need to be monitored, especially during flood or drought events. They are also directly impacted by human activities, through pumping, river embankment, dams, reservoirs, and hydraulic infrastructure. The monitoring of the spatial distribution and temporal variability of surface waters still remains challenging: there could be around 117 million of water bodies with an area above 0.002 km^2 on the continental surfaces according to a recent study (Verpoorter et al., 2014). The biggest lakes and rivers are of course important to the study of global hydrological process and water/carbon cycles. But smaller lakes and rivers begin to draw attention, as they might also play a non-negligible role because of their numbers (e.g. Downing et al., 2010). In situ monitoring of water bodies at global or even regional scales is very heterogeneous, as it depends on local gage networks,. Moreover, in situ measurements are considered sensitive information and are not always freely available to the research community. In this context, satellite measurements are a viable complementary source of information and especially those from nadir altimeters, even if they will not replace in situ measurements.

Initially designed to monitor the dynamic topography of the ocean, satellite radar altimeters have proven their abilities to observe continental surfaces water bodies elevations, allowing long-term observations of water level variations of lakes (e.g., Birkett, 1995; Ponchaut and Cazenave, 1998; Medina et al., 2008; Crétaux et al., 2011; 2015), rivers (e.g., Birkett, 1998; Frappart et al., 2006a; Santos da Silva et al., 2010; Biancamaria et al., 2011; Michailovsky et al., 2012) and floodplains (e.g., Frappart et al., 2005; 2006b; 2012; Lee et al., 2009; Santos da Silva et al., 2010). As altimetry measurements demonstrated their abilities to provide reliable water stages over large water bodies, they started to be used with or to substitute missing in situ data, especially in large remote river basins. Major hydrological applications are currently the followings: calibration of hydrodynamics models (e.g., Wilson et al., 2007; Getirana, 2010; Yamazaki et al., 2012; Paiva et al.,

2013), estimate of discharge using either rating curves (e.g., Kouraev et al., 2004; Papa et al., 2012), routing models (e.g., León et al., 2006; Hossain et al., 2014; Michailovsky and Bauer-Gottwein, 2014), or coupling with measurements of river velocities from multi-spectral images (e.g., Tarpanelli et al., 2015), estimate of surface water storage in large river basins (e.g., Frappart et al., 2012; 2015a), lakes and reservoirs storage dynamics (e.g. Crétaux et al., 2016) and low water maps of the groundwater table (Pfeffer et al., 2014). Nadir altimetry is quite a mature technology, as the very first scientific altimeters flew more than thirty years ago. Continuity of measurements in time is guaranteed by incoming follow-on missions like Jason-3 (launched 17 January 2016), Sentinel-3A (launched 16 February 2016), Sentinel-3B (currently planned for 2017), Sentinel-3C and -3D (which should be launched around 2021; ESA, 2016) and Jason-Continuity of Service/Sentinel-6 (in 2020 for Jason-CS A and 2026 for Jason-CS B; Scharroo et al., 2015).

Radar altimetry, however, has several limitations for monitoring land hydrology. The main restrictions are its low spatial (one measurement every 175 to 400 m along track, for an instrument footprint with several kilometers radius and an intertrack distance at the equator between 80 km to 315 km, depending on the mission) and temporal resolutions (repeat cycle of 10 days for Topex/Poseidon and Jason-1/2/3 missions and 35 days for ERS-1&2, ENVISAT and SARAL, 27 days for Sentinel-3 missions). Because of these limitations, the use of altimetry data has been limited to large (tens of km wide or wider) water bodies. Moreover, altimeters miss most water level extrema during extreme flow periods or fail to study rapid hydrological events such as flash floods. However, the altimeter performance depends not only on river size but also on the surrounding topography (better performance over flat areas), on other surrounding water bodies and, to some extent, on vegetation that will affect the reflected electromagnetic wave (Frappart et al., 2005; Frappart et al. 2006a; Frappart et al., 2006b; Santos da Silva et al., 2010; Crétaux et al., 2011; Ricko et al., 2012).

Improvements in nadir altimetry sensors performance, in the quality of the corrections applied to the altimetry range and in measurements post-processing have allowed measurements of

water stage variations over small-to-medium rivers and small lakes. Small rivers are 40 to 200 m wide, while medium rivers have widths between 200 and 800 m. Small rivers discharge from 10 to 100 $m^3.s^{-1}$ while medium range between 100 and 1000 $m^3.s^{-1}$ (Meybeck et al., 1996). For lakes, small lakes have areas <0.01 km^2 (Verpoorter et al., 2014). On the basis of a global inventory of lakes from optical satellite images, Verpoorter et al. (2014) showed that small lakes are the most numerous (90 million, from a total of 117 million lakes worlwide), but cover a total area (0.27% of non-glaciated land surfaces) much smaller than bigger lakes (which cover a total of 3.5%). Despite their importance for land hydrology and water resources management, a large number of rivers and lakes are poorly gaged (Alsdorf and Lettenmeier, 2003). Few studies have demonstrated the possibility to accurately monitor water levels of small water bodies (e.g., Santos da Silva et al., 2010; Michailovsky et al., 2012; Baup et al., 2014; Frappart et al., 2015a; Sulistioadi et al., 2015). The present study aims at doing this benchmarking for a medium river: the Garonne River in France. Section 2 presents the study domain, in situ gages and radar altimetry missions used. Section 3 compares in situ and altimetry water elevations along the river main course and its estuary, discuss the sources of errors and investigate potential solution for future altimetry missions to improve measurements. Conclusions and perspectives are provided in section 4.

2. Study domain and Methodology

2.1. Garonne River basin presentation and available data

The Garonne River (Figure 1) is located in Southwest France and drains an area of 56,000 km^2. Its mean annual discharge near its outlet, at Tonneins where the river width is around 200 m (Figure 1), is around 600 $m^3.s^{-1}$. At the global scale, according to the Global Runoff Data Center (GRDC) discharge database, it is the 120th largest river in the world by its annual discharge and the 3rd in mainland France. It is therefore a medium river according to Meybeck et al. (1996) (section 1).

The Garonne River has a pluvio-nival regime, with a low flow period between July and

October and high flow period between December and April. The river source is located in the Pyrénées Mountains (South of the basin, Figure 1) and outflows to the Atlantic Ocean via the Gironde estuary. The Garonne supports an agricultural activity that uses 70% of the total water uptake (mainly from surface waters) during low flow period (Sauquet et al., 2009; Martin et al., 2016). For more details on the Garonne basin, see Martin et al. (2016).

Water level and discharge gages on most rivers in France are operated by regional public agencies (DREAL – Directions Régionales de l'Environnement, de l'Aménagement et du Logement) and all their measurements are collected by the Service Central de l'Hydrométéorologie et d'Appui à la Prévision des Inondations (SCHAPI) within the national 'Banque Hydro' database (http://www.hydro.eaufrance.fr). Four gages from this database have been used in this study (Verdun-sur-Garonne, Lamagistère, Tonneins and Marmande, see Figure 1), as they are on the Garonne mainstream and provide validated water level measurements. Data are available with a non-uniform temporal resolution that depends on the water elevation stage (the median time step for all gages in Figure 1 is below 1 hour). All gages have records starting before 01 January 1 2002 (the first year of the oldest altimetry mission considered in this study, see section 2.2.3). Water elevation time series used in this study end 31 December 2010 at Verdun-sur-Garonne, 02 April 2014 at Lamagistère, 01 February 2015 at Tonneins and 28 March 2014 at Marmande. The river width is around 130 m at Verdun-sur-Garonne, 150 m at Lamagistère and 200 m at Tonneins and Marmande. Also, the 15 km reach of the Garonne just upstream of Lamagistère (from the upstream confluence, at Malause, to Lamagistère) has multiple man made hydraulic infrastructures along the river. There are five weirs within the reach and a "run-of-the-river" dam at Malause, which induce river slope breaks. Thus, water elevation variations within this reach and, in particular, at the location of ENV-773 virtual station (see Figure 1 for its location and section 2.2.4 for definition of virtual station), might not be comparable to water elevation variations at Lamagistère gage. There is no similar infrastructure (and no such slope break) near other in situ gages that might impact comparison with altimeter measurements.

Moreover, a Digital Elevation Model (DEM) at 25 m horizontal resolution, with few meters absolute vertical accuracy, is available over the entire mainland France to the research community and provided by the Institut National de l'Information Géographique et Forestière (IGN, http://professionnels.ign.fr), a French government agency which is “the official reference for geographic and forest information in France” (from http://www.ign.fr/institut/en).

Time series for three tide gages are also available on the Gironde estuary, seaward of the Garonne (Figure 1). They are operated by the Service Hydrographique et Océanique de la Marine (SHOM – http://refmar.shom.fr) for the Royan gage (from 19 September 2008 to 31 August 2014) and by the Grand Port Maritime de Bordeaux for Port-Bloc (from 1 January 2006 to 12 October 2014) and Richard (from 1 January 2006 to 31 December 2014) gages, with water level measurements every minute.

All elevations (from gages time series and DEM) are referenced to the “Nouveau Géoréfentiel Français” (NGF-IGN69), the official French vertical reference for the main territory. Because all these data are available, the Garonne River basin is particularly well suited to evaluate the capability of nadir altimeters to observe a medium river between 100 m and 200 m wide.

2.2. Satellite altimetry missions used

2.2.1 Principle of altimetry measurement

The purpose of radar altimeters is to provide the height of the ground surface above a reference ellipsoid. To do so, the altimeter emits a radar pulse and records the radar echo using a pulse compression technique. This record, also known as a waveform, contains the value of the returned power as a function of the distance between the radar and the reflectors. In this study, the term “range” is equivalent to the distance from the instrument. For technical reasons, the altimeter does not record all the power backscattered by all targets between the instrument and the lowest ground elevation within the instrument footprint (all the possible ranges). It only samples a small subset of these ranges, called the range window or tracking window, whose size is typically between 30 m

and 50 or 64 m depending on the instrument, but can reach 1024 m for Envisat in the 20 MHz mode. For more details, see Benveniste et al. (2001), Desjonquères et al. (2010) and Steunou et al. (2015). A special function of the altimeter is to keep the range window tracking the ground surface (see section 2.2.2 for more information related to the on-board tracking system).

The two-way travel-time from the satellite to the surface is the measurement that needs to be estimated as accurately as possible from the waveform. It corresponds to an instant known, in the waveform, as the middle of the leading edge over the ocean. Over other types of surface, this time is more complex to retrieve and depends of the retracking algorithm used. It is accurately determined by the mission ground segment using retracking algorithms and is used to compute the distance between the satellite and the Earth surface, the altimeter range (*R*). Then, the satellite altitude (*H*) referenced to an ellipsoid is computed from orbit modeling, with an accuracy better than 2 cm (e.g. Cerri et al., 2010; Couhert et al., 2015; Dettmering et al., 2015).

Taking into account propagation corrections caused by delays from the interactions of electromagnetic waves in the atmosphere, and geophysical corrections, the height of the reflecting surface (*h*) with reference to an ellipsoid can be estimated as:

$$h = H - \left(R + \sum\left(\Delta R_{propagation} + \Delta R_{geophysical}\right)\right) \quad (1)$$

where *H* is the satellite centre of mass height above the ellipsoid, estimated using the precise orbit determination (POD) technique, *R* is the nadir altimeter range from the satellite center of mass to the surface taking into account instrument corrections, $\sum \Delta R_{propagation}$ is the sum of the geophysical and environmental corrections applied to the range, respectively, and $\sum \Delta R_{geophysical}$ is another geophysical correction. Furthermore, $\sum \Delta R_{propagation}$ is computed as follow:

$$\sum \Delta R_{propagation} = \Delta R_{ion} + \Delta R_{dry} + \Delta R_{wet} \quad (2)$$

where ΔR_{ion} is the atmospheric refraction range delay due to the free electron content associated with the dielectric properties of the ionosphere, ΔR_{dry} is the atmospheric refraction range delay due to the dry gas component of the troposphere, ΔR_{wet} is the atmospheric refraction range delay due to the water vapor and the cloud liquid water content of the troposphere. Also, $\sum \Delta R_{geophysical}$

corresponds to the following corrections:

$$\sum \Delta R_{geophysical} = \Delta R_{solid\ Earth} + \Delta R_{pole} \quad (3)$$

where $\Delta R_{solid\ Earth}$ and ΔR_{pole} are the corrections accounting for crustal vertical motions due to the solid Earth and pole tides, respectively. Over the ocean, other corrections need to be applied to take into account other physical processes (such as ocean tides, see Chelton et al., 2001, for more information).

2.2.2 On board tracking system

As indicated in the previous section, one important function of the altimeter is to modify the position of its tracking window to make it follow the ground topography, which can rapidly change over few kilometers on the continents. This is automatically performed on board in "closed-loop" by the Adaptive Tracking Unit (ATU) from previously received waveforms. Chelton et al. (2001) and Desjonquères et al. (2010) provide a detailed description of the closed-loop tracking system for TOPEX and Poseidon-3 altimeters, respectively. The following paragraph provides only a simplified overview, which is sufficient enough to understand the observations presented in this study.

The principle of the closed loop is that the ATU tries to keep some signal in its tracking window. On Poseidon-3, this is done by using the so-called "median mode" (Desjonquères, 2010), which tries constantly to center the signal in the window. If this fails, the level of received signal decreases dramatically. When the level of received signal becomes lower than a predefined threshold, the ATU considers that the tracking is lost and switches to a "search" mode in which it scans a window, with range of a few kilometers range, centered on the estimated satellite altitude. The scan begins with the smallest range (i.e. closest to the satellite) and the tracking window is moved until the level of received signal exceeds again another specified threshold (Desjonquères et al., 2010).

This behavior implies that the ground surface observed by nadir altimeters heavily depends

261 on the previously received radar echoes. For example, the geometry of the observations can induce
262 loss of radar echoes tracking in some circumstances (e.g., if the satellite trajectory crosses a steep-
263 sided valley perpendicularly) or not, (e.g., if it follows the valley over a long distance). In general,
264 when the tracking is lost and the ATU is in search mode, the signal received from the top of the hills
265 is high enough to exceed the threshold making the ATU to stop the search. This can occur before the
266 tracking window reaches the river that flows in the valley, but of course this depends on the depth
267 of the valley as well as the size of the tracking window. So the top of the hilly areas often tends to
268 be observed rather than rivers in the valley. However the exact behavior of the altimeter depends on
269 the ground reflectivity, the size of the tracking window and the two thresholds mentioned above.
270 Thus, whenever there are variations of topography, there is no way to control which part of the
271 scenery will be observed by the radar altimeter in the closed-loop tracking mode.
272 To overcome this challenge, a new tracking mode, the Doris Immediate Orbit on board
273 DEtermination/Digital Elevation Model (DIODE/DEM) mode, has been implemented on board
274 Poseidon-3 and AltiKa altimeters. In this mode, tracking range is not estimated in closed-loop, but
275 in "open-loop". In this case, the satellite/ground range is not estimated automatically from formerly
276 measured signal, but using a DEM stored on board and an estimate of the satellite orbital position,
277 computed on board and in real time by the DIODE navigator function of the DORIS (Doppler
278 Orbitography and Radio-positioning Integrated by Satellite) instrument (Desjonquères et al., 2010).
279 The DEM mode was activated during cycles 3, 5, 7, 34, 209 and 220 for Jason-2 and only during a
280 portion of SARAL cycle 1 (tracks 600 to 800 from 4 April to 10 April 2013), corresponding to
281 tracks 646 and 773 over the Garonne basin (see Figure 1 for their location). To compute on board
282 elevations used by the DIODE/DEM tracking mode, CNES used an a priori global DEM and a
283 global land/water classification (Desjonquères, 2009). If there is water in the land/water
284 classification within the instrument footprint, then only a priori DEM elevations within the water
285 mask are used to compute on board elevation (Desjonquères, 2009). However, if there is no water,
286 then all land elevations are considered. Therefore, for steep-sided regions with no water in the

classification (or if the water mask is not correctly geolocalized), the computed on board elevations can be closer to the top of the hills elevations than the river valley elevations. Furthermore, the waveform is expected to be centered on the first third of the tracking window. As this window size is around 50 m for Jason-2 and 30 m for SARAL, it has been estimated that the a priori DEM accuracy should be around 10 m (even slightly less for SARAL).

For Jason-2, the a priori global DEM used is the 1 km Altimetry Corrected Elevation DEM (ACE; Berry et al., 2000) and the water mask comes from the Generic Mapping Tools (GMT, http://gmt.soest.hawaii.edu/) (Desjonquères, 2009). A comparison between ACE DEM and 25 m IGN DEM (see section 2.1) tends to show that ACE accuracy over the Garonne valley is better than 10 m. Global-scale ACE uses local Digital Terrain Elevation Data (DTED) and altimetry data from the ERS-1 (European Remote Sensing-1 satellite) acquired during its geodetic mission. However, over the Garonne River valley, ACE elevations come only from DTED (exact source is not provided in the ACE documentation). In addition, the river position in the GMT database is not correctly geolocalized. Therefore, the on board elevations over the Garonne might be biased toward elevations on top of the hills. For SARAL, the a priori global DEM corresponds to ACE2 (Berry et al., 2010) and the land/water mask is derived from Globcover (http://due.esrin.esa.int/page_globcover.php). The accuracy of ACE2 also seems to be better than 10 m over the Garonne valley. Globcover correctly geolocalizes the Garonne River but because of its 300 m pixel size and the undersampling to 1 km pixels in the CNES tool, pixels identified as water do not always correspond to the river surface. These discrepancies can impact the computed elevations stored on board.

Birkett and Beckley (2010) evaluated both the closed-loop and the DIODE/DEM modes (for cycles 3, 5, 7 and 34) for Jason-2 over 28 lakes and reservoirs around the world with areas spanning from 380,000 km^2 (Caspian Sea, Kazakhstan) to 150 km^2 (Windsor lake, Bahamas). They concluded that both modes on Jason-2 are able to monitor water bodies with area around 150 km^2 and width around 0.8 km. This monitoring capability is an improvement compared to

313 Topex/Poseidon and Jason-1, with the DIODE/DEM having the fastest acquisition time for many
314 targets. However, for few targets (Chajih lake, 900 km^2, Windsor lake, 150 km^2, Brokopondo
315 reservoir 1,500 km^2 and Powell and Diefenbaker reservoir systems, 500 km^2 and 550 km^2,
316 respectively), they noted some loss of data in the DIODE/DEM mode for cycles 3, 5 and 7, whereas
317 the closed-loop mode was performing well during other cycles. These targets are better (at least
318 partially) observed during cycle 34, after the on board DEM elevations have been updated and some
319 altimeter parameters have been tuned in cycle 16. They attributed errors to "inadequate resolution
320 and/or data in the DEM" and concluded that the on board DEM might not be "optimized for all
321 regions". For all investigated lakes and reservoirs, they observed some cases where the closed-loop
322 successfully observed the water body, contrarily to the DIODE/DEM. For all other cases, both
323 tracking modes provided similar results (both failed or succeeded to observe water bodies). But
324 there was no case where the DIODE/DEM mode observed the target and the closed-loop did not.
325 However, Birkett and Beckley (2010) considered in their study targets that were larger than the
326 Garonne River.
327
328 **2.2.3 Altimetry datasets**
329 This study uses altimetry missions only after 2002, namely the ENVIronmental SATellite
330 (ENVISAT) mission from the European Space Agency (ESA), Jason-2 mission from National
331 Aeronautics and Space Administration (NASA) and Centre National d'Etudes Spatiales (CNES),
332 and Satellite for ARgos and ALtika (SARAL)/Altimeter in Ka-Band (AlitKa) mission jointly
333 developed by the Indian Space Research Organization (ISRO) and CNES. Table 1 sums up the main
334 characteristics and technical details of these three altimetry missions, which are described in more
335 detail below.
336 ENVISAT mission was launched by ESA on 01 March 2002. It carried 10 instruments
337 including the advanced radar altimeter (RA-2). It was based on the heritage of sensors on board the
338 European Remote Sensing (ERS-1 and 2) satellites. Altimeter RA-2 was a nadir-looking pulse-

limited radar altimeter operating at two frequencies: Ku- (13.575 GHz), as ERS-1 and 2, and S- (3.2 GHz) bands. Its goal was to collect radar altimetry over ocean, land and ice caps (Zelli, 1999). Altimeter RA-2 could change the range resolution to set the range detection window to three sizes: 1024 m, 256 m and 64 m (they are also commonly designated as 20MHz, 80MHz and 320MHz modes, respectively, corresponding to the bandwidths used to achieve the corresponding window width; Benveniste et al., 2001; ESA, 2007). Changing the tracking window is particularly useful over continents to adapt tracking to ground topography changes (regions with rapidly varying altitude will be better tracked with a relatively wider window, whereas flat regions will be more precisely observed with a relatively narrower window). The range window is sampled using a fixed number of bins (or gates). A bin corresponds to a continuous interval of ranges that will be aggregated to a unique range value, during the analog-to-digital conversion step. Changes in range window size are done automatically on board, based on the received signal and reference data stored in the on board memory (ESA, 2007). ENVISAT orbited at an average altitude of 790 km, with an inclination of 98.54°, on a sun-synchronous orbit with a 35-day repeat cycle. It provided observations of the Earth surface (oceans and lands) from 82.4° latitude North to 82.4° latitude South. This orbit was formerly used by ERS-1 and 2 missions, with an equatorial ground-track spacing of about 80 km. ENVISAT remained on this nominal orbit until October 2010 and its mission ended 08 April 2012. This study used ENVISAT data from cycles 6 (which started 14 May 2002) to 94 (which ended 21 October 2010).

Jason-2 mission was launched on 20 June 2008 as a cooperation between CNES, EUMETSAT, NASA and NOAA. Its payload is mostly composed of the Poseidon-3 radar altimeter from CNES, the Advanced Microwave Radiometer (AMR) from JPL/NASA, and a triple system for precise orbit determination: the DORIS instrument from CNES, a GNSS receiver and a Laser Retroflector Array (LRA) from NASA. Jason-2 orbits at an altitude of 1336 km, with an inclination of 66°, on a 10-day repeat cycle, providing observations of the Earth surface (oceans and lands) from 66° latitude North to 66° latitude South, with an equatorial ground-track spacing of about 315

km. This orbit was formerly used by Topex/Poseidon, and Jason-1. Poseidon-3 radar altimeter is a two-frequency altimeter, operating at Ku- (13.575 GHz) and C- (5.3 GHz) bands (Desjonqueres et al., 2010). The tracker range window is the same as previous Poseidon instruments and has a useful size around 50m (sampled over 104 range bins). Jason-2 measurements are used in this study from cycle 1 (which started 12 July 2008) to cycle 227 (which ended 09 September 2014) h. Jason-2 raw data are processed by SSALTO (Segment Sol multimissions d'ALTimétrie, d'Orbitographie).

SARAL is a CNES-ISRO joint-mission that was launched on 25 February 2013. Its payload is composed of the AltiKa radar altimeter and bi-frequency radiometer, and a double system for precise orbit determination (Steunou et al., 2015): DORIS instrument and a Laser Retroflector Array (LRA). SARAL flights on the same nominal orbit than ENVISAT (see above). AltiKa radar altimeter is a mono-frequency altimeter and the first one to operate at Ka-band (35.75 GHz). The bandwidth of the signal has been increased (480 MHz of useful bandwidth; Sengenes and Steunou, 2011) with respect to Jason-2 and ENVISAT, improving the range resolution. As the number of useful bins remains the same as for the Jason altimeters (104 bins), the tracker window size is around 30 m. For electromagnetic wave in Ka-band, ionospheric delay becomes negligible. In this study, SARAL/AltiKa measurements from cycle 1 (which started 14 March 2013) to cycle 17 (which ended 30 October 2014) have been used.

Altimetry data processed in this study come from the Geophysical Data Records (GDRs) – GDR T patch 2 for SARAL, GDR v2.1 for ENVISAT, GDR D for Jason-2, delivered by CNES/ESA/NASA processing centers. Since this study has been performed, a new Jason-2 GDR version has been released in May 2015 (GDR E). Differences between GDR D and E are expected to have a low impact on the results presented here, as the foreseen improvement is a better agreement of the geographically correlated radial orbit drift rate (1 mm/year to less than 0.5 mm/year over roughly 6 years) with respect to JPL (RLSE14A) GPS-only reduced-dynamic orbits for Jason-2 (for more details, see http://www.aviso.altimetry.fr/fileadmin/documents/data/tools/New_GDR_E_orbit_20150521.pdf).

391 Similarly, a new SARAL GRD E is now available. But SARAL GDR T patch 2 and SARAL GDR
392 E must provide similar results for this study. These data are provided in a consistent NetCDF
393 (Network Common Data Form) format with coherent geophysical corrections for all missions by
394 Centre de Topographie de l'Océan et de l'Hydrosphère (CTOH –http://ctoh.legos.obs-mip.fr/). They
395 are sampled along the altimeter track at 18, 20 and 40 Hz for ENVISAT, Jason-2 and SARAL
396 respectively. As explained in the previous section, a so-called retracker algorithm is needed to
397 estimate the satellite/ground range R (Eq. 1) and the surface backscattering coefficient from the
398 received electromagnetic signal. Previous studies showed that Ice-1 retracking algorithm (Wingham
399 et al., 1986) is one of the most suitable for hydrological studies, in terms of accuracy of water levels
400 and availability of the data (e.g. Frappart et al., 2006a; Santos da Silva et al., 2010), among the
401 commonly available retracked data present in the GDRs. However, Santos da Silva et al. (2010)
402 found, on the Amazon basin, that Ice-2 retracking algorithm (Legrésy and Rémy, 1997) could
403 provide similar results to Ice-1. Sulistioadi et al. (2015) showed, for some 250 m wide Indonesian
404 river reaches, that Sea Ice retracking algorithm (Laxon, 1994) can provide, in some cases, slightly
405 more accurate water levels than Ice-1. In the following, when not explicitly indicated, ranges used
406 to derive altimeter heights and backscattering coefficients are those derived from the Ice-1
407 retracking algorithm. ENVISAT GDRs directly provide ranges estimated using Ice-1 and Sea Ice
408 algorithms. Therefore, in section 3.1, a comparison is presented between Ice-1 and Sea Ice derived
409 water heights for ENVISAT measurements. Ice-2 retracker has not been considered as it provides
410 similar results to Ice-1 (Santos da Silva et al., 2010). Similarly, the retracker used over ocean
411 (Brown, 1977) has not been used, as it has been widely shown that it provides the worst results
412 compared to the three other retracking algorithms for rivers (e. g. Frappart et al., 2006a; Santos da
413 Silva et al., 2010; Sulistioadi et al., 2015).
414 Over the ocean, wet troposphere corrections are computed from the on board radiometer
415 measurements, for each altimetry mission. However, measurements over continents from these
416 radiometers cannot be used to estimate those corrections, as the ground emissivity (contrarily to

water) is much more important than the emissivity from the atmosphere. In this case, the propagation corrections applied to the range are derived from the Era Interim model outputs by the European Centre Medium-Range Weather Forecasts (ECMWF) for the dry/wet troposphere range delays. The range correction accounting for ionosphere delays is estimated using the Global Ionospheric Maps (GIM).

2.2.4 Time series of altimetry-based water levels

Time variations of river levels from radar altimetry measurements are computed at virtual stations. A virtual station is defined as the intersection between an orbit ground track and a water body (*i.e.*, lake, reservoir river channel, floodplain or wetland). At these specific locations, variations from one cycle to the next of height *h*, derived from altimeter measurements (see Eq. 1), can be associated to changes in water level.

In this study, we used the Multi-mission Altimetry Processing Software (MAPS) that allows a refined selection of the valid altimetry data to build virtual stations (Frappart et al., 2015b). Data processing is composed of three main steps: a coarse delineation of the virtual stations using Google Earth, a refined selection of the valid altimetry data, and a computation of the water level time-series. For virtual stations on the Garonne mainstream (Figure 1), the length of the selection is not constant and varies from 700 m to 2 km. The altimetry-based water level is computed for each cycle using the median of the selected altimetry heights, along with their respective deviation (*i.e.*, mean absolute deviations). This process is repeated each cycle to construct the water level time series at the virtual stations.

3. Results

3.1. Multi-satellite water elevation on the Garonne River mainstream

The altimetry-based time series of water elevation at virtual stations shown on Figure 1 have been compared to the closest in situ station available in the Banque Hydro database (see section

2.1), with the exception of virtual stations JA2-070a and JA2-070b. They have not been used in this study, as the confluence with the Lot River (one of the main Garonne River tributaries) is located between the closest in situ gage (Tonneins) and the virtual stations. Therefore water elevation at the gage might not be representative of water elevation at the virtual stations.

For other virtual stations, only common dates have been used for the comparison between altimetry and in situ time series. In situ measurements recorded the same day as the altimetry measurement are linearly interpolated at the altimetry measurement observation time. If there is no in situ measurement the same day as the altimetry observation, this observation is not considered. In situ time series have been referenced to UTC (Coordinated Universal Time) to match the altimeter time reference. Elevation anomaly time series have been computed for both the altimeters and in situ gages. The anomalies are computed by removing, from the elevation time series, its temporal mean over the same common dates between in situ and altimetry time series (e.g. Biancamaria et al., 2011).

Table 2 shows the correlation coefficient, mean bias (mean of the difference) and Root Mean Square Error (RMSE) between altimetry and in situ time series for both absolute water elevations referenced to NGF-IGN69 and water elevation anomalies, along the Garonne River mainstream. For anomaly time series, the Nash-Sutcliffe (NS) coefficient (Nash and Sutcliffe, 1970) is also computed. The NS coefficient, which ranges between $-\infty$ and 1, is widely used to assess how an estimated time series (most of the time from a model) accurately match (i.e., in time and amplitude) in situ measurements. The closer to 1 the NS coefficient is, the closest to the in situ time series the altimetry-based water elevations are. NS above 0.5 can be considered satisfactory (Moriasi et al., 2007). However, a negative NS means that the estimated time series is a worse “predictor” than the in situ time series mean and should be considered as unacceptable (Moriasi et al., 2007). In this study, the NS is not computed for absolute water elevation (bias between absolute in situ and altimetry water elevation induces negative NS), but for their anomalies. Table 2 also provides distance between the altimetry virtual station and the gage, number of common dates between

altimetry and in situ time series, and the amplitude (maximum minus minimum over the common dates) of the in situ time series.

At Lamagistère and Verdun-sur-Garonne, ENVISAT data are not really correlated to the in situ measurement and the NS coefficients are negative, indicating poor performance of the altimeters. For virtual stations ENV-102 and ENV-773, which correspond to the worst results for ENVISAT, the distance to the in situ gage can partially explain the mismatch. However, the small river width (~150 m) and the surrounding topography affecting the quality of the altimetry signal are also likely to be an important source of error. Virtual station ENV-646, which is only 1 km downstream the gage at Lamagistère, has better RMSE (1.80 m for absolute water elevations and 0.80 for water elevation anomalies), correlation coefficient (0.61) and NS coefficient (-0.53) compared to upstream ENVISAT virtual stations, even if they cannot be considered as satisfactory.

Downstream, at Tonneins and Marmande, where the river width is around 200 m, ENVISAT altimetry time series are of good quality with correlation coefficient around 0.8, NS around 0.7 and water elevation anomalies RMSE between 0.5 m and 0.6 m for ENVISAT. For ENVISAT and Jason-2, the mean bias must be mostly explained by the river slope between the gage and the altimetry virtual station, as they have the same order of magnitude as the slopes computed from IGN DEM, even if the DEM vertical accuracy (few meters) prevents a quantitative estimate of the river slope (which also varies in time). The sign of the bias depends of the position of the virtual station compared to the gage (positive if the virtual station is downstream and negative if it is upstream). Yet, some part of this bias might also be related to the altimeter measurement error.

Results shown in Table 2 have been computed using Ice-1 retracker algorithm and the median value of altimetry heights for each observation time (see section 2.2.4). Even if some studies reported better results using Ice-1 retracker (over the Amazon see Frappart et al., 2005; Frappart et al., 2006a; Santos da Silva et al., 2010), Sulistioadi et al. (2015) found that Ice-1 was not always providing the best results for some Indonesian rivers, whose widths were around 250 m. In this study, the Sea Ice retracker was sometimes performing better than Ice-1. As ENVISAT GDRs

provide ranges computed using at least these two retracker algorithms, we computed water elevation from both retrackers and compared them to in-situ measurements for ENVISAT virtual stations along the Garonne mainstream. These results are shown in Table 3. Within each virtual station, the median water elevation is computed for each observation time, as it is more robust than the mean, when there are outliers (Frappart et al., 2005; Frappart et al., 2006a). However, Santos da Silva et al. (2010) stated that computing both the median and the mean can provide a "qualitative indicator of the presence of outliers". That is why both the median and the mean are shown in Table 3. This table seems to confirm the results from Sulistioadi et al. (2015), the best results are not always obtained with Ice-1. For the three virtual stations with NS coefficient below 0, two have better results with Sea Ice. For the two virtual stations with NS coefficient above 0.5, one has better results with Ice-1, the other with Sea Ice. However, for these two virtual stations, difference between RMSE for these two retrackers is just a few centimeters, which is small compared the actual value of the RMSE (more than 50 cm). Therefore, both retrackers are well suited for the Garonne basin. Results using the median are better, most of the time, than results using the mean (except for Ice-1 and virtual station ENV-315, where the RMSE using the mean is only 2 cm lower than the RMSE using the median). From these results it seems that both the median Ice-1 and the median Sea Ice are well suited for the Garonne basin. Differences between these two retrackers are one order of magnitude lower than the RMSE obtained from comparison to in situ time series.

Figure 2 shows enlargements from Figure 1 on ENVISAT and Jason-2 virtual stations at Lamagistère (a.), at Tonneins (b.) and in the estuary (c.). Especially, it should be recalled that there are four weirs between ENV-773 virtual station and Lamagistère gage (as explained in section 2.1), which are 10 km apart. These weirs cause slope breaks and can explain at least a part of the 1.55 m water elevation anomalies RMSE for this virtual station. Figure 3 shows ENVISAT (red curves for Ice-1 and cyan curves for Sea Ice) and in situ (blue curves) water elevation anomaly time series at the satellite measurement times for virtual stations ENV-646 (Fig 3.a) and ENV-188 (Fi. 3.c). On this figure, the right panels (b. and d.) show all records in the in situ water elevation anomalies time

series (blue dots) and the altimetry water elevation anomaly measurements (red dots for Ice-1 and cyan dots for Sea Ice) during the common time period for these two virtual stations. These right panels highlight the coarse altimetry time sampling. On Figure 3.d, ENVISAT seems to roughly sample the water elevation seasonal cycle, but, because of the 35 days repeat orbit, it cannot observe intra-monthly variability. This variability can be quite important for a medium river like the Garonne, for which precipitation and snow melting induce few meters water elevation variations within few days at Tonneins. Figure 3 corresponds to two virtual stations (ENV-646 and ENV-188) for which Sea Ice retracker is performing better than Ice-1 retracker, yet the two retrackers time series remain close. Table 3 shows that for two other virtual stations (ENV-773 and ENV-315) Ice-1 performs better than Sea Ice. This result is in agreement with the results obtained by Sulistioadi et al. (2015): for medium size rivers, Ice-1 is not always the best retracker. However, water elevation obtained from both retrackers are close enough and both could be used (there is just few centimeters difference between them for the two virtual stations, which have a correlation coefficient above 0.8). According to these results and as Sea Ice retracker is not provided in Jason-2 GDRs, only results using Ice-1 retracker will be shown in the following.

For Jason-2 virtual station JA2-070, in between Tonneins and Marmande, correlation coefficient is equal to 0.98, NS around 0.95 and the RMSE of water elevation anomalies is close to 20 cm. Results for virtual stations JA2-035 show slightly lower agreement with a correlation coefficient of 0.91 and water elevation anomalies RMSE and NS coefficient of 0.36 cm and 0.82, respectively. The most noticeable feature in this virtual station is the few dates (62) that measure river water commonly with the Marmande gage time series (Table 2). In comparison, virtual station JA2-070 has 150 dates with measurements of river water elevation during the same period. For the other dates, elevations are 50 m higher than valid measurements of river water elevations and have therefore been removed during the virtual station time series generation before comparison with in situ data. These dates (around 40 for JA2-070 and 140 for JA2-035) correspond to cases when the altimeter remains ‘locked’ on the surrounding hills (see section 2.2.2 for an explanation of this

phenomenon). The Garonne valley is roughly 5 km or less wide at these locations and is surrounded by hilly areas (see Figure 2) that can be 50 m to 100 m higher than the valley (according to the IGN DEM and knowledge of the region). These two virtual stations also illustrate the importance of the geometry of observation. The track 070 is almost parallel to the valley over a long distance (almost 30 km). Therefore, distance variations between the ground and the radar are much smoother compared to the track 035 that crosses the valley almost orthogonally.

Figure 4 presents similar plots than Figure 3, but for the Jason-2 virtual station JA2-070, using Ice-1 retracker only (red curves and red dots). This virtual station clearly shows better results than ENVISAT virtual station ENV-188 (Figure 3.c and 3.d), when compared to Tonneins in situ time series. Besides, with a 10 days repeat orbit, Jason-2 observes higher frequency variations, but still misses all the local maxima and especially the 2009 and 2014 heavy floods, which lasted only few days.

Table 2 also highlights high mean bias for most SARAL virtual stations, only virtual station SRL-188 have correlation and errors similar to ENVISAT. For the three other ones, the mean error goes from 44 m to 105 m, with few dates in the time series, indicating that the altimeter is not observing the river valley but the surrounding hills. This problem is similar to that already observed for Jason-2 time series. However, for these SARAL virtual stations and contrary to Jason-2 virtual stations, there is no measurement on the river. ENVISAT is less affected by such effects, thanks to its three resolutions (see section 2.2.3) and differences in the closed-loop parameters. This drawback and potential reasons for the differences between the three missions is discussed in more detail in section 3.2.

In the Gironde estuary, at Richard tide gage (see Figure 1 for its location), both ENVISAT and SARAL tracks 274 compare unfavorably to in situ measurements (Table 4) with correlation coefficients of 0.28 and 0.09, respectively. As the absolute vertical reference for this tide gage is not known, mean bias and the absolute elevation RMSE cannot be computed. The RMSE of water elevation anomalies is around 1.5 m. Differences between altimetry and in situ time series could be

related to instrument error, impact of surrounding lands and the fact that water elevation variations at the tide gage might not be representative of water elevation variations along the satellite ground track. Figure 5, shows the measured elevation from ENVISAT/RA2 for track 274 during 21 June 2007 (red line) and the IGN DEM elevation (green curve) on the estuary. It shows that over half of the estuary, the altimeter remains locked over the surrounding topography (which is a common issue for nadir altimetry due to the closed-loop tracking mode, as explained in section 2.2.2). These measurements are not taken into account to compute time series for ENV-274, but represent a source of error that is likely to affect the altimetry signal in the lower estuary.

Results are much better for both ENVISAT and SARAL tracks 859 (Table 4) at Port-Bloc and Royan tide gages (see Figure 1 and 2.c for their locations). The correlation coefficient is above 0.97, water elevation anomalies RMSE are around 30 cm for ENVISAT and 10 cm for SARAL. The comparison between anomalies time series measured by Port-Bloc tide gage and ENVISAT track 859 is shown on Figure 6.a and 6.b and SARAL track 859 on Figure 6.c and 6.d. Figures 6.b. and 6.d. also highlight the well-known effect of tidal aliasing in the altimeter water elevation time series, due to the altimetry satellite orbit repeat period which is much higher than the tides period (e. g. Le Provost, 2001). As stated by Le Provost (2001), the important difference between altimeter time sampling (10 days or 35 days) and semidiurnal and diurnal tides period (between 12 to 24 hours), leads to alias these tides “into periods of several months to years”. But the issue of tidal aliasing is beyond the scope of the present paper.

3.2. Tracking issue and possible solution

The challenge of observing the Garonne valley for some altimetry mission (SARAL/AltiKa, but also Jason-2 and ENVISAT to a lower extent), highlighted in section 3.1, has multiple origins, as explained in section 2.2.2. The Garonne valley is only 5 km wide at virtual stations ENV-/SRL-773 and 50 m to 100 m lower than the surrounding hilly areas. Due to the closed-loop tracking algorithm, nadir altimeter tends to get locked on the top of the hilly areas and miss steep-sided

599 valleys (see section 2.2.2). The portion of SARAL/AltiKa ground track that crosses the Garonne
600 valley (roughly perpendicularly, see Figure 2.a) is only 7 km long. As the antenna footprint on the
601 ground is equal to 4 km, considering the 3-dB aperture angle of 0.6° for SARAL that defines the
602 half-power points of the antenna radiation pattern (Steunou et al., 2015), the instrument still
603 receives some backscattered energy from the surrounding hilly areas for previous radar echoes
604 when it is near and over the valley. Therefore, the ATU does not change the position of the tracking
605 window, which remains locked on the hills. After few kilometers, the hills are not in the antenna
606 footprint anymore and no more energy is received, resulting in a loss of measurements. By the time
607 the instrument changes the tracking window position (search mode, see section 2.2.2) and receives
608 again some energy, acquisition of the Garonne valley has been lost. Figure 7 shows an example of
609 data loss by AltiKa due to the closed-loop. On this figure, the x-axis represents the latitude along
610 the SARAL track 773 (see Figure 2.a for its location) and the y-axis corresponds to elevation
611 referenced to NGF-IGN69. The green curve corresponds to the IGN DEM. The Garonne River
612 location is indicated by the blue rectangle. SARAL measurement for cycle 2 (in closed-loop) is
613 shown by the magenta dashed line. During cycle 2, AltiKa remains locked over the hills and loses
614 tracking over the Garonne valley, as previously explained.

615 Signal-locking over hills is less frequent for Jason-2 virtual station JA2-070, because of a
616 more favorable observation configuration than SARAL. Jason-2 track flies over the Garonne valley
617 and follows the river over 30 km before virtual station JA2-070. Therefore, elevation variations
618 observed by the satellite are smoother than SARAL. Smoother variations along Jason-2 track allow
619 more time for the closed-loop tracking algorithm to adapt to the hills/valley transition, whereas
620 ENVISAT and SARAL track 188 is almost perpendicular to the valley (Figure 2.b). Jason-2 virtual
621 station JA2-035 has a configuration of observation close to SARAL track 188, that is why it also
622 has few river water elevation measurements.

623 However, ENVISAT better performance compared to SARAL/AliKa is not due to a different
624 observation configuration (contrary to Jason-2, as SARAL is on the same orbit), but it must be

related to the three window sizes that are chosen automatically on board (64 m, 256 m, 1024 m, see section 2.2.3). ENVISAT is better suited to observe ground with appreciable slope variations as the instrument increases the size of its tracking window, which allows measurements in the river valley. Table 5 shows percentage of data for all ENVISAT cycles acquired with each window size, for all virtual stations. Measurements for virtual stations close to high relief have more tracking window size variability (typically the case of ENV-102, ENV-773 and ENV-315). At ENV-188 virtual station, the river is more distant from high relief, the altimeter is very frequently in 320 MHZ mode (64 m window size) and that is also why it is the only SARAL/AltiKa virtual station observing river water elevations. However, increasing the tracking window size (with the same number of range bins) degrades the range resolution of the altimeter. Yet, SARAL better results over the estuary, compared to ENVISAT, must be linked to its improved range resolution.

Nadir altimeters observe a ground surface most of the time but this surface is not always the most useful for hydrologists. To overcome this issue and force the altimeter to observe the river valley instead of the surrounding hilly areas, the DIODE/DEM tracking mode has been developed by CNES (see section 2.2.2). SARAL/AltiKa measurements for virtual station SRL-773 were performed in DIODE/DEM mode during the first cycle of the mission and they are shown in Figure 7 (red curve). In this mode, AltiKa successfully observes the Garonne valley without data loss and does not remain locked over the hills, despite the terrain steepness (highest terrain slopes are around 80 m/km at 44.05°N and 100 m/km at 44.06°N).

Measurements for track 773 show the potential of the DEM mode to let the altimeter observe a river within a steep-sided valley. Yet, this mode requires that the a priori DEM stored on board has better accuracy than the size of the tracking window. For track 646, the on board DEM value is almost 40 m above the actual Garonne valley elevation. This discrepancy can be related to the Globcover classification, used in combination with ACE DEM, to compute on board elevations (see section 2.2.2). Around virtual station SRL-646, there is no water pixel on the Garonne River in Globcover (contrary to virtual station SRL-773), which biases on board elevation toward the top of

651 the hills elevation. Therefore, AltiKa loses signal over the Garonne even for cycle 1. A similar
652 discrepancy occurs with Jason-2 cycles in DEM mode. For this altimeter mission, the GMT water
653 mask used is not correctly geolocalized on the river (section 2.2.2). Thus, elevations computed
654 along the satellite track and loaded on board are also close to the top of the surrounding hills
655 elevations and not the river valley. Therefore, these cycles provide similar results to the Jason-2
656 cycles in closed-loop, which remains locked on the top of the hills for both track 070 and 035. This
657 example clearly shows DEM tracking mode sensitivity to the databases (a priori DEM and water
658 mask) used to compute the on board elevations, especially if the tracking window is smaller.
659
660 **3.3. Observation of a narrow artificial canal**
661 A frequent question asked about nadir altimetry concerns the minimum water body size that
662 can be observed with this type of altimeter. It is impossible to answer this question generally. From
663 previous examples shown in this study, it is clear that the main reasons explaining why a water body
664 is observed or not at a specific time is more linked with previous waveform history, instrument
665 settings, ground topography rather than just the water body size. The previous example of the
666 SARAL track 773 for cycle 1 on the Garonne River is a good example of such situation. All water
667 bodies within the instrument footprint that backscatter enough energy will be observed in one or
668 multiple range gates (if they are in the tracking window). In this case, the waveform will have
669 multiple peaks (with different amplitudes), corresponding to these water bodies. They could also be
670 observed on multiple consecutive waveforms along the satellite ground track. Retrackers, like Ice-1
671 used in this study, use the whole waveform measured by the altimeter within the tracking window to
672 estimate one range value. Therefore, Ice-1 provides elevation for only one observed water body (the
673 first peak), but not for the others.
674 To account for the heterogeneity of the scene observed by the altimeter and all the potential
675 targets measured by the instrument, it is beneficial to plot the radargram, which corresponds to
676 waveforms recorded by the altimeter along the satellite track around a virtual station. The radargram

for virtual station SRL-773 during cycle 1 (in DIODE/DEM tracking mode) is shown in Figure 8. This figure shows the history of the returned power along the track over the virtual station. The x-axis corresponds to time (or along-track latitude) and the y-axis to the range gate number (equivalent to distance). The intensity of the returned power (normalized to the maximum power registered during the pass, in decibels) is shown by the color. The parabolic shapes observed on this figure are characteristic of the signal returned by small size water bodies. The returned signal is received by the altimeter a few kilometers before and after the satellite crosses the river. The variation of distance between the river and the radar during this period explains the parabolic shape (closest approach corresponds to the minimum of the parabola). Two examples of such observations in Figure 8 are caused by the Garonne River and the narrow artificial canal. Two other points can also be observed and correspond to very high intensity of the received signal. These points also correspond to bright targets and the absence of parabola associated to them is caused by the nature of the retrodiffusion by these targets: they are very specular in contrast to the two points previously discussed. For more information on diffusive and specular targets responses in a radargram, see, for example, Tournadre et al. (2006). Figure 2.a shows specifically SARAL track 773 for cycle 1 (dashed red line) and the overflown water bodies near SRL-773 virtual stations. This specific track is 1.5 km shifted compared to the nominal ENVISAT/SARAL track, due to some less stringent requirement on the satellite position during the first cycles. From Figure 2.a, it is clear that the first specular target and the first diffusive target corresponds to the Southernmost lake/reservoir and the Garonne River mainstream (southernmost channel on this figure, which is ~150 m wide) of the image, respectively. The second diffusive target, which is higher than the Garonne mainstream, corresponds to the artificial canal (northernmost channel, ~70 m wide), which brings cooling water to the Golfech nuclear power plant. It is less clear what the second specular target is (it could be another smaller lake/reservoir, a bright man made structure like a road or metallic building roofs or even another much smaller artificial canal : the “canal du Midi”). Positions of the Garonne River and the Golfech canal along SARAL track are also indicated on Figure 7 (blue polygons).This

example clearly shows that nadir altimeters can observe small targets (river or canal with width below 100 m), when the tracking window is correctly set.

4. Conclusion and perspectives

Nadir altimeters have proven their capability to observe water elevation for major rivers (like the Amazon, the Congo, etc.). In this study, it has been shown they can also provide meaningful water elevation for a 200 m wide, steep-sided river: the lower Garonne River in France. Jason-2 time series measures water elevation with 20 cm RMSE compared to in situ observations at Tonneins (115 km upstream the estuary), whereas ENVISAT mission had higher RMSE (50 cm) compared to the same in situ gage. With good reason, Jason-2 10-day repeat orbit is better suited to observe Garonne River seasonal cycle than the ENVISAT 35-day orbit. Therefore, Jason-2 (and to a lower extent ENVISAT) repeat period seems appropriate to observe water level variations at the seasonal cycle, annual, interannual and even decadal time scale (since Jason-2 was launched in 2008). However, Jason-2 time sampling is too coarse for observing daily/hourly high frequency water level variations for this kind of medium size river. The Garonne River is very sensitive to short-time intense rain events and quick snowmelt, which induces several meters water elevation variations in few days and all these rapid events are missed by the satellite altimeters. Upstream Tonneins, ENVISAT has higher errors and does not seem to measure water elevation as accurately (Jason-2 does not sample the river upstream).

Comparisons between ENVISAT and in situ water elevations showed that Ice-1 retracker and Sea Ice retracker provide very similar results when the Garonne River is around 200 m-wide, confirming what was obtained by Sulistioadi et al. (2015). This is due to the peaky shape of the waveform for small and medium size water bodies. When studying drainage basins with various river widths, it would be better to use only Ice-1 altimeter heights for consistency between the altimetry-based time series of water levels. Ice-1 retracking algorithm provides much better results than Sea Ice over large rivers and wetlands. Ice-1-derived altimeter ranges are available in the GDR

729 for all recent altimetry missions, which is not currently the case for Sea Ice.

730 SARAL/AlitKa mostly fails to observe the river valley and remains locked on the hilly
731 surrounding areas. Such problem also happens with ENVISAT, but less often. It also happens quite
732 frequently for the Jason-2 virtual station downstream of Marmande (the other one near Tonneins is
733 less affected). This issue is related mainly to the closed-loop tracking algorithm which is influenced
734 by the history of the measurements and the geometry of observation. As a consequence, over the
735 continents, nadir altimeters tend to be locked over the top of the topography within the instrument
736 footprint and during previous measurements. This is the case over the Garonne River for
737 SARAL/AltiKa and for Jason-2 track 035, which crosses the narrow (~5 km) and steep-sided
738 Garonne River valley almost perpendicularly. However, over 30 km, Jason-2 track 70 is almost
739 parallel to the river and within the valley, which allows the closed-loop tracking mode to get locked
740 on the river. ENVISAT provides more measurements on the river, not because of a different
741 observation geometry (SARAL has the same orbit as ENVISAT), but because of differences in
742 closed-loop tracking parameters and its three tracking window sizes. Different window sizes help
743 sample a wider range span. Over the estuary, SARAL/AltiKa provides smaller RMSE (around 10
744 cm) than ENVISAT (around 30 cm) compared to tide gages.

745 To overcome challenges inherent to closed-loop tracking mode that tends to observe top of
746 the topography instead of steep-sided river, an experimental tracking mode has been developed by
747 the CNES: the DIODE/DEM mode. For SARAL/AltiKa, this experimental mode has been activated
748 only during the first cycle. Over the Garonne River, it successfully observed the Garonne valley for
749 track 773, whereas for other cycles, in closed-loop tracking mode, it failed to observe it. Yet, this
750 mode requires a priori DEM values (derived from ACE2 for SARAL) and land/water mask (derived
751 from Globcover for SARAL) to compute DEM on board along the satellite track. This on board
752 computed DEM must have vertical accuracy better than the tracking window size (which is
753 typically in the range 30-50 m, see section 2.2.2), otherwise it provides incorrect tracking
754 commands and misses the river valley (like for SARAL track 646 cycle 1 and Jason-2 track 070 and

035 cycles in DEM tracking mode over the Garonne). Therefore, for this tracking mode, it is crucial to have an a priori, validated, database of the expected elevation for all water bodies the altimeter will be forced to observe, with vertical accuracy better than the size of the tracking window. The on board DEM is highly dependent of both input water mask and DEM used, which should be consistent among themselves. On board DEM can be improved by using satellite imagery (e.g. Landsat) for more accurate water mask, like the NARWidth database (Allen and Pavelsky, 2015). For DEM values, it should be assessed if and where current global DEM are compatible with the used water mask (e.g. elevations around the water mask should be lower than surrounding topography in steep-sided valleys) and accurate enough. Using new (or soon to be released) improved DEM, like the new version of Shuttle Radar Topography Mission (SRTM) DEM (released in September 2014, see http://www2.jpl.nasa.gov/srtm/) or the DLR global TanDEM-X DEM (Zink et al., 2014), should also improve computed on board DEM.

Therefore, the DIODE/DEM mode seems promising for future altimetry missions to observe previously missed steep-sided rivers (or lakes). However, performance, benefits and limits of this mode for continental hydrology will require more investigation by the scientific community, especially because two new altimetry satellites have just been launched (Jason-3, 17 January 2016, and Sentinel-3A, 16 February 2016). These altimeters are equipped with the DIODE/DEM mode available along with the closed-loop tracking mode.

Acknowledgements

This project was funded by the “Réseau Thématique de Recherche Avancée - Sciences et Technologies pour l’Aéronautique et l’Espace” (RTRA STAE), through a grant attributed to the “Ressources en Eau sur le bassin de la GARonne : interaction entre les composantes naturelles et anthropiques et apport de la téléDétection” (REGARD) project.

IGN, SCHAPI (especially Etienne Le Pape), DREAL Midi-Pyrénées (especially Didier Narbaïs-Jaureguy), SHOM and “Grand Port Maritime de Bordeaux” (especially Alain Fort) are

gratefully thanked for providing freely all the DEM, in situ data and ancillary information used in this study.

CTOH observation service at LEGOS (http://ctoh.legos.obs-mip.fr/) is also acknowledged for processing and providing altimetry data in a uniform format for all missions.

CNES, ESA, ISRO and NASA are acknowledged for providing freely to the scientific community measurements from the ENVISAT/RA2, Jason-2/Poseidon-3 and SARAL/AltiKa altimeters.

Three anonymous reviewers are thanked for their constructive comments that helped to improve this paper.

References

Alsdorf, D. E., and D. P. Lettenmaier. 2003. "Tracking fresh water from space." *Science* 301: 1491–1494.

Allen, G. H., and T. M. Pavelsky. 2015. "Patterns of river width and surface area revealed by the satellite-derived North American River Width data set." *Geophysical Research Letters* 42: 395–402. doi:10.1002/2014GL062764.

Baup, F., F. Frappart, and J. Maubant. 2014. "Combining high-resolution satellite images and altimetry to estimate the volume of small lakes." *Hydrology and Earth System Sciences* 18: 2007-2020. doi:10.5194/hess-18-2007-2014.

Benveniste, J., M. Roca, G. Levrini, P. Vincent, S. Baker, O. Zanife, C. Zelli, and O. Bombaci. 2001. "The Radar Altimetry Mission: RA-2, MWR, DORIS and LRR." ESA bulletin 106: 67-76, http://www.esa.int/esapub/bulletin/bullet106/bul106_5.pdf (last accessed, 19 July 2016)

807 Berry, P.A.M., R. Hilton, C.P.D. Johnson, and R.A. Pinnock. 2000. “ACE: a new GDEM
808 incorporating satellite altimeter derivedheights”. *Proceedings of the ERS-EnvisatSymposium,*
809 *Gothenburg, Sweden,* ESA SP-461., 783-791.
810
811 Berry, P. A. M., R. G. Smith, and J. Benveniste. 2010. “ACE2: the new Global Digital Elevation
812 Model.” In *Gravity, Geoid and Earth Observation: IAG Commission 2: Gravity Field, Chania,*
813 *Crete, Greece, 23-27 June 2008*, edited by P. S. Mertikas, 231-237. Berlin-Heidelberg: Springer.
814 isbn: 978-3-642-10634-7. doi: 10.1007/978-3-642-10634-7_30.
815
816 Biancamaria, S., F. Hossain, and D. P. Lettenmaier. 2011. “Forecasting transboundary river water
817 elevations from space.” *Geophysical Research Letters* 38: L11401. doi:10.1029/2011GL047290.
818
819 Birkett, C. M. 1995. “The contribution of TOPEX/POSEIDON to the global monitoring of
820 climatically sensitive lakes.” *Journal of Geophysical Research: Oceans* 100: 25179-25204.
821
822 Birkett, C. M. 1998. “Contribution of the TOPEX NASA radar altimeter to the global monitoring of
823 large rivers and wetlands.” *Water Resources Research* 34(5): 1223–1239.
824
825 Birkett, C. M., and B. Beckley. 2010. “Investigating the Performance of the Jason-2/OSTM Radar
826 Altimeter over Lakes and Reservoirs.” *Marine Geodesy*, 33(S1): 204-238.
827 doi:10.1080/01490419.2010.488983.
828
829 Brown, G.S. 1977. “The average impulse response of a rough surface and its applications”. IEEE
830 Transactions on Antennas and Propagation 25(1): 67-74. doi:10.1109/TAP.1977.1141536.
831
832 Cerri, L, J.-P. Berthias, W.I. Bertiger, B.J. Haines, F.G. Lemoine, F. Mercier, and J.C. Ries. 2010.

833 “Precision Orbit Determination Standards for the Jason Series of Altimeter Missions.” *Marine*
834 *Geodesy* 33(Suppl.):379-418. doi:10.1080/01490419.2010.488966.
835
836 Chelton, D.B., J.C. Ries, B.J. Haines, L.-L. Fu, and P.S. Callahan. 2001. “Satellite Altimetry”. In
837 *Satellite altimetry and Earth Sciences*, edited by Fu, L.-L. and A. Cazenave, 27-32. San Diego:
838 Academic Press.
839
840 Couhert, A., L. Cerri, J.-F. Legeais, M. Ablain, N.P. Zelensky, B.J. Haines, F.G. Lemoine, W.I.
841 Bertiger, S.D. Desai, and M. Otten. 2015. “Towards the 1 mm/y stability of the radial orbit error at
842 regional scales.” Advances in Space Research 55(1):2-23. doi:10.1016/j.asr.2014.06.041.
843
844 Crétaux, J. F., W. Jelinski, S. Calmant, A. V. Kouraev, V. Vuglinsk, M. Bergé Nguyen, M.-C.
845 Gennero, F. Niño, R. A. Del Rio, A. Cazenave, and P. Maisongrande. 2011. “SOLS: A lake database
846 to monitor in the Near Real Time water level and storage variations from remote sensing data”.
847 *Advances in Space Research* 47 (9): 1497-1507. doi:10.1016/j.asr.2011.01.004.
848
849 Crétaux, J.-F., S. Biancamaria, A. Arsen, M. Bergé-Nguyen, and M. Becker. 2015. “Global surveys
850 of reservoirs and lakes from satellites and regional application to the Syrdarya river basin”.
851 *Environmental Research Letters* 10(1): 015002. doi:10.1088/1748-9326/10/1/015002.
852
853 Crétaux, J.-F., R. A. Abarca-del-Río, M. Bergé-Nguyen, A. Arsen, V. Drolon, G. Clos, and P.
854 Maisongrande. 2016. “Lake Volume Monitoring from Space”. *Surveys in Geophysics* 1-37.
855 doi:10.1007/s10712-016-9362-6.
856
857 Dettmering, D., C. Schwatke, and W. Bosch. 2015. “Global Calibration of SARAL/AltiKa Using
858 MultiMission Sea Surface Height Crossovers.” Marine Geodesy 38(sup1):206-218.

doi:10.1080/01490419.2014.988832.

Desjonquères, J.D. 2009. “POSEIDON3 DEM/Diode Coupling Mode”. 2009 OSTST meeting, Seattle, USA, http://www.aviso.altimetry.fr/fileadmin/documents/OSTST/2009/oral/Desjonqueres_coastal.pdf (last accessed, 22 July 2016)

Desjonquères, J.-D., G. Carayon , N. Steunou, and J. Lambin. 2010. “Poseidon-3 Radar Altimeter: New Modes and In-Flight Performances”. *Marine Geodesy* 33(S1): 53-79. doi:10.1080/01490419.2010.488970

Downing, J. A. 2010. “Emerging global role of small lakes and ponds: little things mean a lot”. *Limnetica* 29(1): 9-24.

ESA. 2007. *ENVISAT RA2/MWR Product Handbook* 2.2. http://envisat.esa.int/handbooks/ra2-mwr/CNTR.html (last accessed, 9 February 2016)

ESA. 2016. “EC/ESA COPERNICUS - SENTINEL-3C AND -3D MODELS PROCUREMENT”. *ESA Intended Invitation To Tender*, A0 n°1-8197, http://emits.sso.esa.int/emits/owa/emits_iitt.show_iitt?actref=15.156.03&user=Anonymous (last accessed, 22 March 2016)

Frappart, F., F. Seyler, J. M. Martinez, J. G. León, and A. Cazenave. 2005. “Floodplain water storage in the Negro River basin estimated from microwave remote sensing of inundation area and water levels.” *Remote Sensing of Environment* 99:387-399. doi:10.1016/j.rse.2005.08.016.

885 Frappart, F., S. Calmant, M. Cauhopé, F. Seyler, and A. Cazenave. 2006a. “Preliminary results of
886 ENVISAT RA-2 derived water levels validation over the Amazon basin.” *Remote Sensing of the*
887 *Environment* 100(2): 252–264. doi:10.1016/j.rse.2005.10.027.
888
889 Frappart, F., K. Do Minh, J. L’Hermitte, A. Cazenave, G. Ramillien, T. Le Toan, and N. M.
890 Mognard-Campbell. 2006b. “Water volume change in the lower Mekong basin from satellite
891 altimetry and imagery data.” *Geophysical Journal International* 167(2): 570–584.
892 doi:10.1111/j.1365-246X.2006.03184.x.
893
894 Frappart, F., F. Papa, J. Santos da Silva, G. Ramillien, C. Prigent, F. Seyler, and S. Calmant. 2012.
895 “Surface freshwater storage and dynamics in the Amazon basin during the 2005 exceptional
896 drought.” *Environmental Research Letters* 7: 044010. doi:10.1088/1748-9326/7/4/044010.
897
898 Frappart, F., F. Papa, Y. Malbeteau, J. G. León, G. Ramillien, C. Prigent, L. Seoane, F. Seyler and S.
899 Calmant. 2015a. “Surface freshwater storage variations in the Orinoco floodplains using multi-
900 satellite observations.” *Remote Sensing* 7(1): 89-110. doi:10.3390/rs70100089.
901
902 Frappart, F., F. Papa, V. Marieu, Y. Malbeteau, F. Jordy, S. Calmant, F. Durand, and S. Bala. 2015b.
903 “Preliminary Assessment of SARAL/AltiKa Observations over the Ganges-Brahmaputra and
904 Irrawaddy Rivers.” *Marine Geodesy* 38(sup1): 568-580. doi:10.1080/01490419.2014.990591.
905
906 Frappart, F., C. Fatras, E. Mougin, V. Marieu, A. Diepkilé, F. Blarel, and P. Borderies. 2015c.
907 “Radar altimetry backscattering signatures at Ka, Ku, C, and S bands over West Africa”. *Physics*
908 *and Chemistry of the Earth, Parts A/B/C* 83-84: 96-110. doi:10.1016/j.pce.2015.05.001.
909
910 Getirana, A. 2010. “Integrating spatial altimetry data into the automatic calibration of hydrological

models". *Journal of Hydrology* 387(3-4): 244–255. doi:10.1016/j.jhydrol.2010.04.013.

Hossain, F., A. H. M Siddique-E-Akbor., L. C. Mazumdar, S. M. Shah Newaz, S. Biancamaria, H. Lee, and C. K. Shum. 2014. "Proof of concept of an operational altimeter-based forecasting system for transboundary flow." *IEEE Journal of Selected Topics in Applied Earth Observations and Remote Sensing* 7(2): 587-601. doi:10.1109/JSTARS.2013.2283402.

Kouraev, A., E. A. Zakharov, O. Samain, N. M. Mognard-Campbell, and A. Cazenave. 2004. "Ob' river discharge from Topex/Poseidon satellite altimetry." *Remote Sensing of Environment* 93: 238-245. doi:10.1016/j.rse.2004.07.007.

Laxon, S. 1994. "Sea ice altimeter processing scheme at the EODC". *International Journal of Remote Sensing* 15(4): 915-924.

Le Provost, C. 2001. "Ocean tides". In *Satellite altimetry and Earth Sciences*, edited by Fu, L.-L. and A. Cazenave. San Diego: Academic Press

Lee, H., C. Shum, Y. Yi, M. Ibaraki, J.-W. Kim, A. Braun, C.-Y. Kuo, and Z. Lu. 2009. "Louisiana wetland water level monitoring using retracked TOPEX/POSEIDON altimetry." *Marine Geodesy* 32: 284-302. doi:10.1080/01490410903094767.

Legrésy, B., and F. Rémy. 1997. "Surface characteristics of the Antarctic ice sheet and altimetric observations". *Journal of Glaciology* 43(144): 197-206.

León, J.G., S. Calmant, F. Seyler, M. P. Bonnet, M. Cauhopé, F. Frappart, N. Filizola, and P. Fraizy. 2006. "Estimation of stage-discharge rating curves and mean water depths from radar altimetry data

and hydrological modelling in the upper Negro River basin." *Journal of Hydrology* 328(3-4): 481-496. doi:10.1016/j.jhydrol.2005.12.006.

Martin, E., S. Gascoin, Y. Grusson, C. Murgue, M. Bardeau, F. Anctil, S. Ferrant, R. Lardy, P. Le Moigne, D. Leenhardt, V. Rivalland, J.-M. Sánchez Pérez, S. Sauvage, and O. Therond. 2016. "On the use of hydrological models and satellite data to study the water budget of river basins affected by human activities: examples from the Garonne basin of France." Surveys in Geophysics 37(2): 223-247. doi:10.1007/s10712-016-9366-2.

Medina, C. E., J. Gomez-Enri, J. J. Alonso, and P. Villares. 2008. "Water level fluctuations derived from ENVISAT Radar Altimeter (RA-2) and in situ measurements in a subtropical waterbody: Lake Izabal (Guatemala)." *Remote Sensing of Environment* 112(9): 3604-3617. doi:10.1016/j.rse.2008.05.001.

Meybeck, M., G. Friedrich, R. Thomas, and D. Chapman. 1996. "Chapter 6 - Rivers." In *Water Quality Assessments – a Guide to Use of Biota, Sediments and Water in Environmental Monitoring*, 2nd Edn., edited by D. Chapman, UNESCO/WHO/UNEP, 247-248. London-New York: Taylor and Francis.

Michailovsky, C. I., S. McEnnis, P. A. M. Berry, R. Smith, and P. Bauer-Gottwein. 2012. "River monitoring from satellite radar altimetry in the Zambezi River basin." *Hydrology and Earth System Sciences* 16: 2181–2192. doi:10.5194/hess-16-2181-2012.

Michailovsky, C. I., and P. Bauer-Gottwein. 2014. "Operational reservoir inflow forecasting with radar altimetry: the Zambezi case study." *Hydrology and Earth System Sciences* 18(3): 997-1007. doi:10.5194/hess-18-997-2014.

963

964 Moriasi, D.N. , J. G. Arnold, M. W. Van Liew, R. L. Bingne, R. D. Harmel, and T. L. Veith. 2007.
965 "Model evaluation guidelines for systematic quantification of accuracy in watershed simulations."
966 *Transactions of the ASABE* 50(3): 885-900.

967

968 Nash, J. E., and J. V. Sutcliffe. 1970. "River flow forecasting through conceptual models part I-A
969 discussion of principles." *Journal of Hydrology* 10(3): 282-290. doi:10.1016/0022-1694(70)90255-
970 6.

971

972 Paiva, R. C. D., D. C. Buarque, W. Colischonn, M.-P. Bonnet, F. Frappart, S. Calmant, and C. A. B.
973 Mendes. 2013. "Large-scale hydrological and hydrodynamics modelling of the Amazon River
974 basin." *Water Resources Research* 49(3):1226-1243. doi:10.1002/wrcr.20067.

975

976 Papa, F., S. K. Bala, R. Kumar Pandey, F. Durand, A. Rahman, and W. B. Rossow. 2012. "Ganga-
977 Brahmaputra river discharge from Jason-2 radar altimetry: an update to the long-term satellite-
978 derived estimates of continental freshwater forcing flux into the Bay of Bengal." *Journal of*
979 *Geophysical Research* 117: C11021. doi:10.1029/2012JC008158.

980

981 Pfeffer, J. , F. Seyler, M.-P. Bonnet, S. Calmant, F. Frappart, F. Papa, R. C. D. Paiva, F. Satgé, and J.
982 Santos da Silva. 2014. "Low-water maps of the groundwater table in the central Amazon by satellite
983 altimetry." *Geophysical Research Letters* 41: 1981–1987. doi:10.1002/2013GL059134.

984

985 Ponchaut, F., and A. Cazenave. 1998. "Continental lake level variations from Topex/poseidon
986 (1993-1996)." *Comptes Rendus de l'Académie des Sciences Series IIA Earth and Planetary Science*
987 326(1): 13-20.

988

989 Ricko, M., C. Birkett, J. A. Carton, and J.-F. Crétaux. 2012. “Intercomparison and validation of
990 continental water level products derived from satellite radar altimetry.” *Journal of Applied Remote*
991 *Sensing* 6(1): 061710. doi:10.1117/1.JRS.6.061710.
992
993 Santos da Silva, J., S. Calmant, F. Seyler, O. Corrêa Rotunno Filho, G. Cochonneau, and
994 W. J. Mansur. 2010. “Water levels in the Amazon basin derived from the ERS 2 and ENVISAT
995 radar altimetry missions.” *Remote Sensing of Environment* 114: 2160–2181.
996 doi:10.1016/j.rse.2010.04.020.
997
998 Sauquet, E, A. Dupeyrat, F. Hendrickx, C. Perrin, R. Samie, J.-P. Vidal. 2009. *IMAGINE 2030,*
999 *climat et aménagements de la Garonne : quelles incertitudes sur la ressource en eau en 2030 ?*
1000 [IMAGINE 2030, climate and water management: uncertainties on water resources for the Garonne
1001 river basin in 2030?]. Lyon: Irstea Publications. http://cemadoc.irstea.fr/oa/PUB00028876-imagine-
1002 2030-climat-amenagements-garonne-quelles-i.html (last accessed 23 February 2016).
1003
1004 Scharroo, R., H. Bonekamp, C. Ponsard, F. Parisot, A. von Engeln, M. Tahtadjiev, K. de Vriendt,
1005 and F. Montagner. 2015. “Jason continuity of services: continuing the Jason altimeter data records
1006 as Copernicus Sentinel-6.” *Ocean Science Discussion* 12: 2931-2953. doi:10.5194/osd-12-2931-
1007 2015.
1008
1009 Sengenes, P., and N. Steunou. 2011. “SARAL/ALTIKA”. 2011 OSTST meeting, San Diego, USA,
1010 http://www.aviso.oceanobs.com/fileadmin/documents/OSTST/2011/oral/03_Friday/Plenary/New%2
1011 0Frontiers/05%20Pierre%20SARAL-AltiKa%20San%20Diego%20OSTST%202011%2021-10-
1012 2011.pdf (last accessed, 22 July 2016)
1013
1014 Steunou, N., J.-D. Desjonquères, N. Picot, P. Sengenes, J. Noubel, and J. C. Poisson. 2015. “AltiKa

1015 Altimeter: Instrument Description and In Flight Performance." *Marine Geodesy* 38(sup1): 22-42.
1016 doi: 10.1080/01490419.2014.988835.
1017
1018 Sulistioadi, Y. B., K.-H. Tseng, C. K. Shum, H. Hidayat, M. Sumaryono, A. Suhardiman, F.
1019 Setiawan, and S. Sunarso. 2015. "Satellite radar altimetry for monitoring small rivers and lakes in
1020 Indonesia." *Hydrology and Earth System Sciences* 19: 341-359. doi:10.5194/hess-19-341-2015.
1021
1022 Tarpanelli, A., L. Brocca, S. Barbetta, M. Faruolo, T. Lacava, and T. Moramarco. 2015. "Coupling
1023 MODIS and radar altimetry data for discharge estimation in poorly gauged river basins." *IEEE*
1024 *Journal of Selected Topics in Applied Earth Observations and Remote Sensing* 8(1): 141-148.
1025 doi:10.1109/JSTARS.2014.2320582.
1026
1027 Tournadre, J., B. Chapron, N. Reul, and D. C. Vandemark. 2006. "A satellite altimeter model for
1028 ocean slick detection." *Journal of Geophysical Research* 111:C04004. doi:10.1029/2005JC003109.
1029
1030 Verpoorter, C., T. Kutser, D. A. Seekell, and L. J. Tranvik. 2014. "A global inventory of lakes based
1031 on high-resolution satellite imagery." *Geophysical Research Letters* 41: 6396–6402.
1032 doi:10.1002/2014GL060641.
1033
1034 Wilson, M.D., P. D. Bates, D. E. Alsdorf, B. Forsberg, M. Horrit, J. Melack, F. Frappart, J. S.
1035 Famiglietti. 2007. "Modeling large-scale inundation of Amazonian seasonally flooded wetlands."
1036 *Geophysical Research Letters* 34: L15404. doi:10.1029/2007GL030156.
1037
1038 Wingham, D.J., C. G. Rapley, and H. Griffiths. 1986. "New techniques in satellite altimeter
1039 tracking systems". In *Proceedings of IGARSS'86 Symposium, Zürich, 8–11 September*
1040 *1986*, edited by ESA, SP-254: 1339–1344.

Yamazaki, D., H. Lee, D. E. Alsdorf, E. Dutra, H. Kim, S. Kanae, and T. Oki. 2012. “Analysis of the water level dynamics simulated by a global river model: A case study in the Amazon River.” *Water Resources Research* 48: W09508. doi:10.1029/2012WR011869.

Zelli, C. 1999. “ENVISAT RA-2 advanced radar altimeter: instrument design and prelaunch performance assessment review.” *Acta Astronautica* 44 (7): 323–333. doi:10.1016/S0094-5765(99)00063-6.

Zink, M., M. Bachmann, B. Bräutigam, T. Fritz, I. Hajnsek, A. Moreira, B. Wessel, G. Krieger. 2014. “TanDEM-X: The new global DEM takes shape.” *IEEE Geoscience and Remote Sensing Magazine*, 2 (2), 8-23. doi:10.1109/MGRS.2014.2318895.

Tables

Table 1. Altimetry missions used in this study and their main characteristics

	Altimetry missions used		
Mission name	ENVISAT	Jason-2	SARAL
Operating agencies	ESA	CNES, EUMETSAT, NASA, NOAA	CNES, ISRO
Mission duration	2002 - 2010 on the nominal orbit (below)	2008 - present	2013 - present
Orbit repeat period	35 days	10 days	35 days
Orbit altitude	790 km	1336 km	790 km
Orbit inclination	98.54°	66°	98.54°
Equatorial ground-track distance	80 km	315 km	80 km
Altimeter name	RA-2	Poseidon-3	AtiKa
Radar frequencies	Ku- and S-bands	Ku- and C-bands	Ka-band
Range window size	64 m, 256 m, 1024 m	50 m	30 m
Number of used range window bins	104	104	104
Along track sampling	18 Hz (~400 m)	20 Hz (~350 m)	40 Hz (~175 m)
DEM tracking mode	No	Yes	Yes
DEM used for DEM mode	-	ACE	ACE2
Cycle(s) in DEM tracking mode	-	3, 5, 7, 34, 209, 220	1

Table 2. Satellite altimetry virtual stations name, closest in situ gage name, number of common dates in the altimetry and in situ time series, correlation coefficient, mean bias and RMSE between altimetry and in situ water elevation time series, RMSE and Nash-Sutcliffe coefficient between altimetry and in situ water elevation anomaly time series, and amplitude (maximum minus minimum) of the in situ water elevation time series at the common dates, along the Garonne River mainstream (from upstream to downstream virtual stations).

Alti virtual station (+ length river crossing)	In situ gage (+ river width in m)	Dist alti/gage (km)	Nb dates alti/ in situ	Corr coeff	Mean bias (m)	RMSE (m)	Anom RMSE (m)	Anom NS coeff	In situ amplitude (m)
ENV-102 (250 m)	Verdun-sur-Garonne (130 m)	29.5	48	0.41	27.90	27.92	0.95	-3.10	1.56
ENV-773 (130 m)	Lamagistère (150 m)	10.5	46	0.35	8.66	8.80	1.55	-2.63	3.52
SRL-773 (130 m)	Lamagistère (150 m)	10.5	6	-0.80	105.10	105.13	2.56	-3.88	3.29
ENV-646 (175 m)	Lamagistère (150 m)	1.4	64	0.62	1.61	1.80	0.81	-0.53	2.60
SRL-646 (175 m)	Lamagistère (150 m)	1.4	6	-0.14	103.53	103.55	2.01	-2.00	3.29
ENV-188 (700 m)	Tonneins (200 m)	2.5	70	0.85	-0.23	0.58	0.53	0.73	3.83
SRL-188 (700 m)	Tonneins (200 m)	2.5	11	0.90	-1.77	1.90	0.69	0.80	5.3
JA2-070 (185 m)	Tonneins (200 m)	5.3	165	0.98	-2.56	2.57	0.22	0.95	4.41
JA2-070 (185 m)	Marmande (200 m)	9.2	150	0.98	4.04	4.04	0.20	0.96	4.20
ENV-315 (2 km)	Marmande (200 m)	14.2	21	0.81	-1.27	1.41	0.59	0.66	3.43
SRL-315 (2 km)	Marmande (200 m)	14.2	4	-0.84	44.15	44.19	1.97	-1.36	3.48
JA2-035 (160 m)	Marmande (200 m)	30	62	0.91	-6.95	6.96	0.36	0.82	3.74

Table 3. Correlation coefficient, RMSE (in meter) and Nash-Sutcliffe coefficient between water elevation anomaly time series for ENVISAT altimetry and the closest in situ gage (see Table 2), along the Garonne River mainstream (from upstream to downstream virtual stations). The comparison is done for two retracker algorithms (Ice-1 and Sea Ice) and using rather the median or the mean of retracked points within the virtual station per observation time. In bold number correspond to the better result obtain for each virtual station and each statistic.

		ENVISAT virtual stations				
		ENV-102	ENV-773	ENV-646	ENV-188	ENV-315
Corr coeff	Median Ice-1	0.42	**0.35**	0.63	0.85	0.82
	Mean Ice-1	0.41	0.35	0.62	0.85	**0.84**
	Median Sea Ice	**0.50**	0.33	**0.65**	**0.88**	0.79
	Mean Sea Ice	0.50	0.33	0.65	0.87	0.80
Anom RMSE (m)	Median Ice-1	0.95	**1.55**	0.81	0.53	0.59
	Mean Ice-1	0.94	1.55	0.80	0.54	**0.57**
	Median Sea Ice	**0.89**	1.80	**0.70**	**0.51**	0.63
	Mean Sea Ice	0.89	1.80	0.69	0.51	0.61
Anom NS coeff	Median Ice-1	-3.10	**-2.63**	-0.53	0.73	0.66
	Mean Ice-1	-3.01	-2.63	-0.48	0.72	**0.69**
	Median Sea Ice	**-2.60**	-3.90	-0.12	**0.76**	0.62
	Mean Sea Ice	-2.60	-3.90	**-0.09**	0.75	0.65

Table 4. Satellite altimetry virtual stations name, closest tide gage name, number of common dates in the altimetry and in situ time series, correlation coefficient, mean bias and RMSE between

altimetry and in situ water elevation time series, RMSE and Nash-Sutcliffe coefficient between altimetry and in situ water elevation anomaly time series, and amplitude (maximum minus minimum) of the in situ water elevation time series at the common dates, along the Gironde estuary.

Alti virtual station	Tide gage	Dist alti/gage (km)	Nb dates alti/ in situ	Corr coeff	Mean bias (m)	RMSE (m)	Anom RMSE (m)	Anom NS coeff	In situ amplitude (m)
ENV-274	Richard	6.5	35	0.28	-	-	1.51	-0.91	5.26
SRL-274	Richard	6.5	15	0.09	-	-	1.57	-0.21	4.54
ENV-859	Royan	5.0	17	0.98	1.01	1.06	0.31	0.94	3.76
SRL-859	Royan	5.0	15	0.99	0.32	0.34	0.09	0.99	3.27
ENV-859	Port-Bloc	3.7	39	0.97	0.73	0.78	0.26	0.94	3.55
SRL-859	Port-Bloc	3.7	15	0.99	0.14	0.20	0.13	0.98	3.26

Table 5. Percentage of data, for all ENVISAT cycles, acquired in each tracking mode, for all virtual stations. 320 MHz, 80 MHz and 20 MHz tracking modes correspond to a tracking window size of 64 m, 256 m and 1024 m, respectively.

		ENVISAT virtual stations						
		ENV-102 (river)	ENV-315 (river)	ENV-773 (river)	ENV-646 (river)	ENV-188 (river)	ENV-274 (estuary)	ENV-859 (estuary)
ENVISAT tracking modes	320 MHz	28	77	44	76	80	96	100
	80 MHz	71	22	33	23	19	3	0
	20 MHz	0	1	23	1	1	1	0

Figures

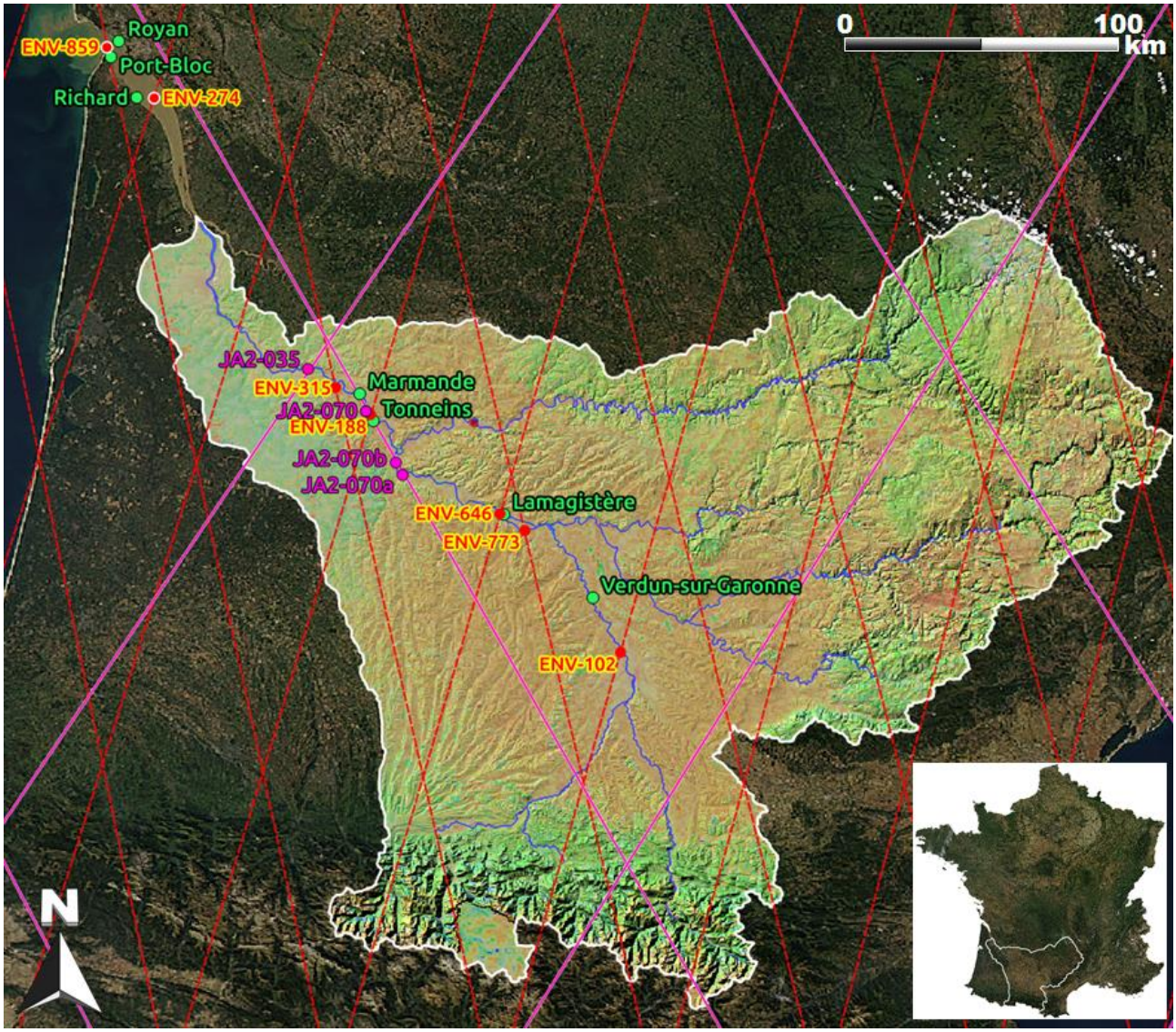


Figure 1. Garonne basin (white boundaries), with in situ gages (green dots), ENVISAT and SARAL virtual stations (red dots) and Jason-2 virtual stations (magenta dots) used in this study. Dotted red lines correspond to ENVISAT and SARAL ground tracks. Magenta lines correspond to Jason-2 ground tracks. Background colors correspond to a MODIS image from 01 October 2011, whose color has been artificially lightened using a shaded relief, computed from a DEM provided by IGN, over the Garonne basin. Location of the Garonne basin in France main territory is shown in the bottom right hand corner map (white boundaries)

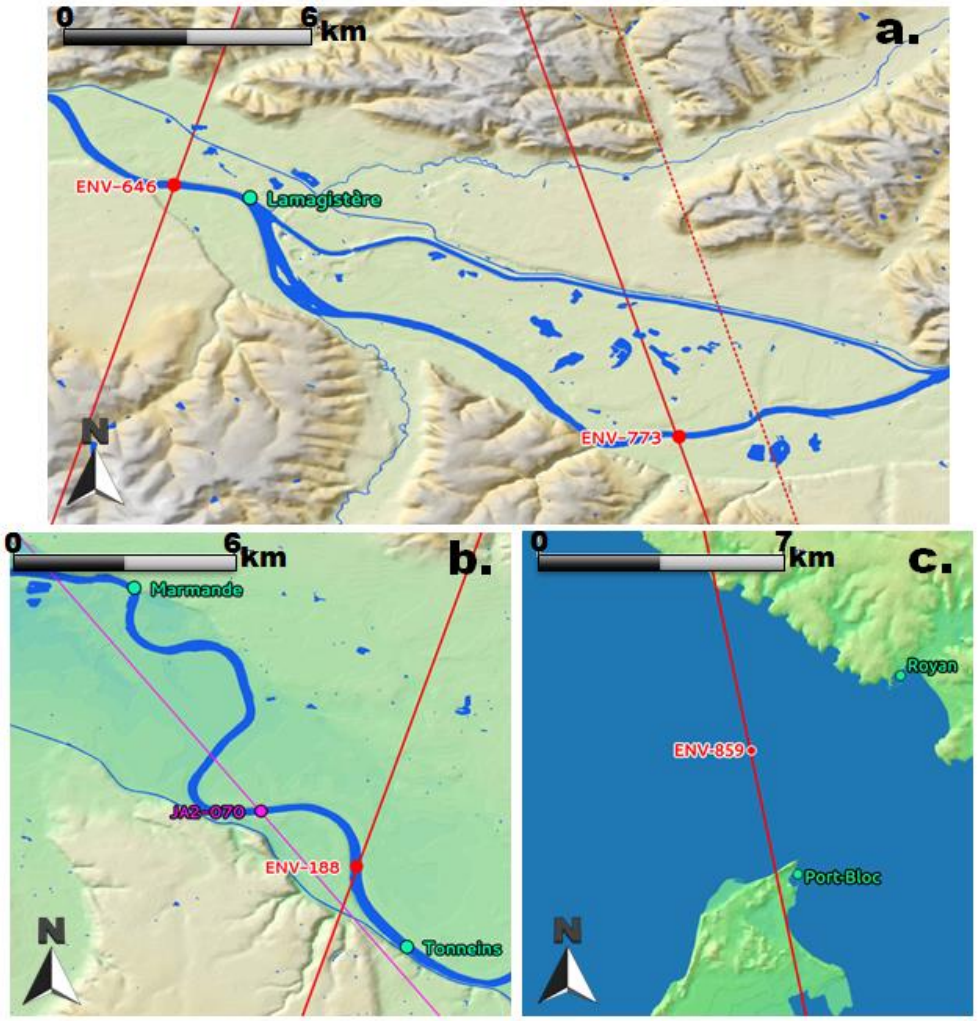


Figure 2. ENVISAT satellite nominal ground tracks (red line), ENVISAT virtual stations (red dots), Jason-2 satellite nominal ground track (magenta), Jason-2 virtual stations (magenta dot) and in situ gages (green dots) over the Garonne mainstream at Lamagistère (a.), Tonneins (b.) and over the estuary (c.). Dashed red line on panel (a.) corresponds to SARAL ground track 773 for cycle 1

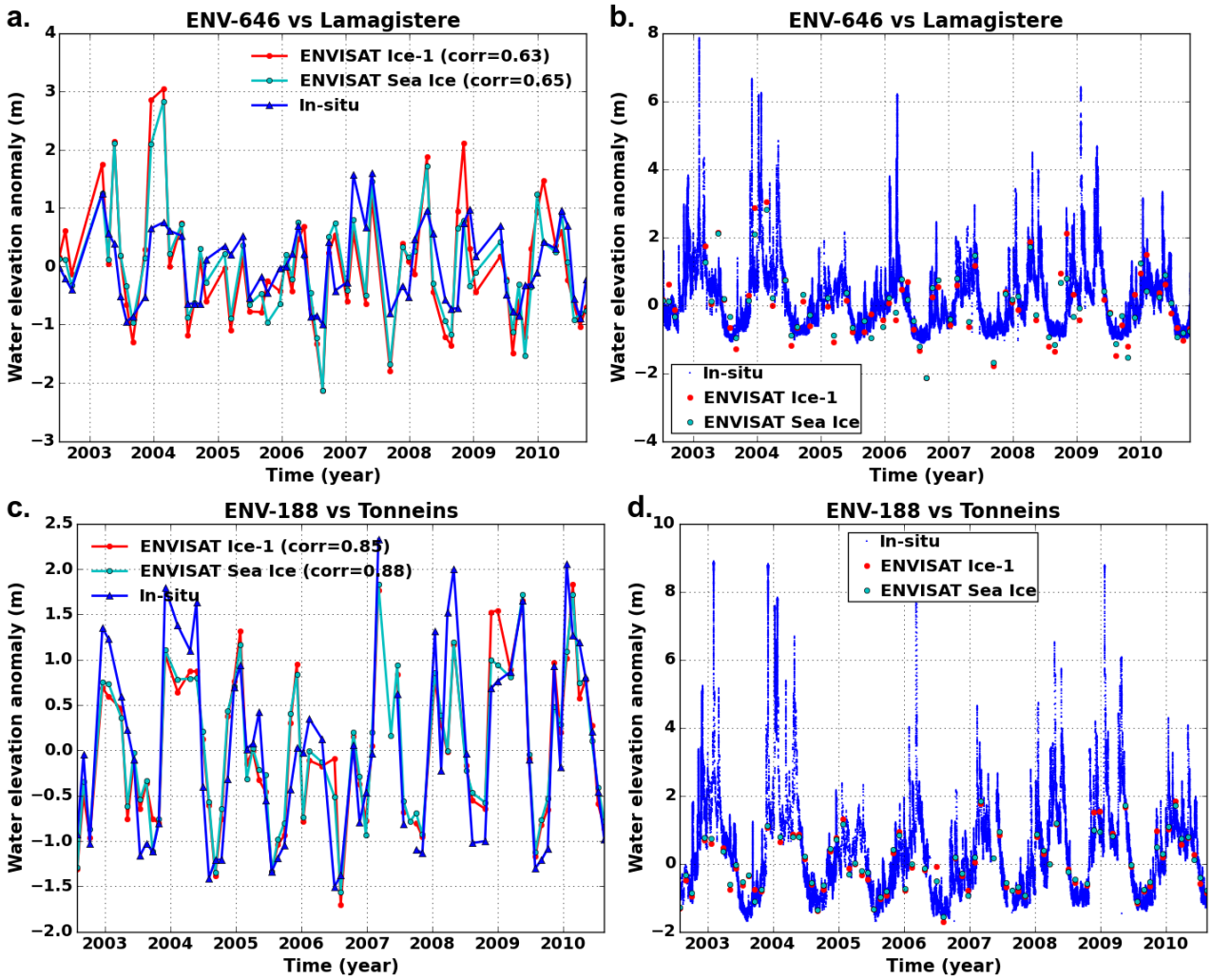


Figure 3. ENVISAT water elevation anomaly computed with Ice-1 retracker (red line on panels a. and c. and red dots on panels b. and d.) and with Sea Ice retracker (cyan line on panels a. and c. and cyan dots on panels b. and d.), in situ water elevation anomaly at ENVISAT measurement times (blue line on panels a. and c.) and all records in the in situ water elevation anomaly time series between 2003 and 2010 (blue dots on panels b. and d.) for virtual station 646 and Lamagistère gage (panels a. and b.) and virtual station 188 and Tonneins gage (panels c. and d.). In these panels, water elevation anomaly time series correspond to water elevations minus the time series temporal mean over the same common dates between in situ and altimetry time series. The term 'corr' corresponds to the altimetry time series and the corresponding in situ time series correlation coefficient. For more statistics concerning these virtual stations, see Table 2

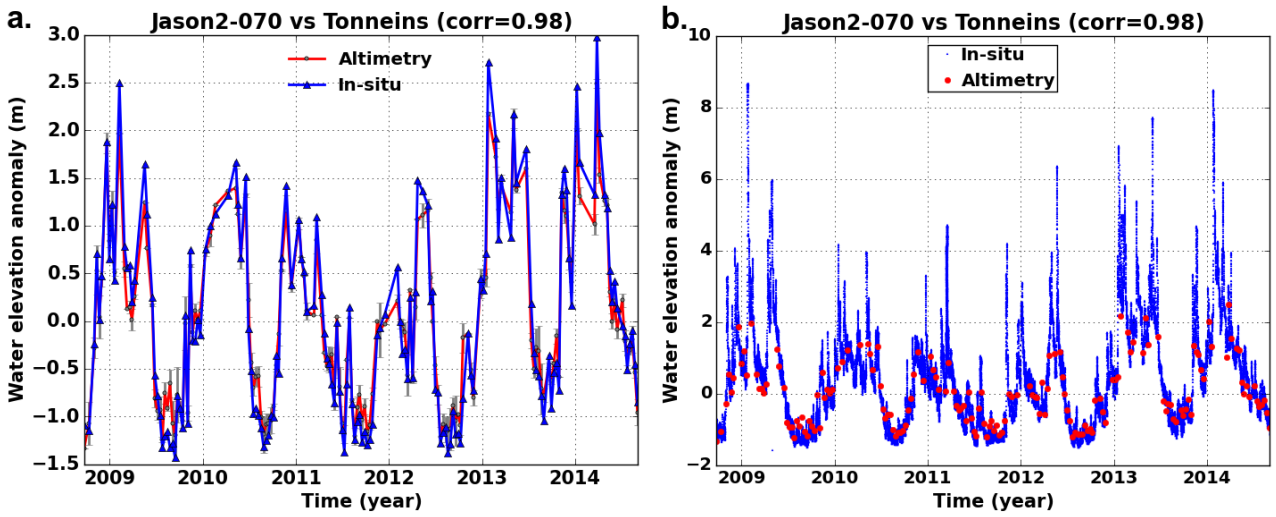


Figure 4. Jason-2 virtual station 070 water elevation anomaly (red line on panel a. and red dots on panel b.) and in situ water elevation anomaly measured by the Tonneins gage at Jason-2 measurement times (blue line on panel a.) and all records in the in situ water elevation anomaly time series between 2003 and 2010 (blue dots on panel b.)

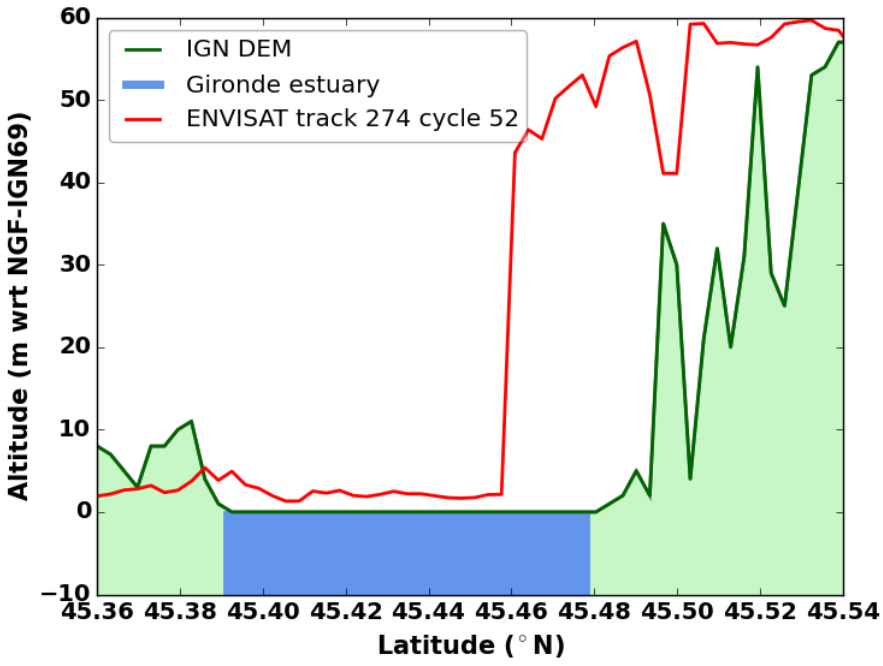


Figure 5. Comparison between IGN DEM (green line) along the ENVISAT 274 track (see Figure 1) over the Gironde estuary (its position is shown by the light blue polygon, its elevation corresponds to the DEM and not to the actual water level) and elevation measured by ENVISAT for cycle 59 (21

June 2007, red curve)

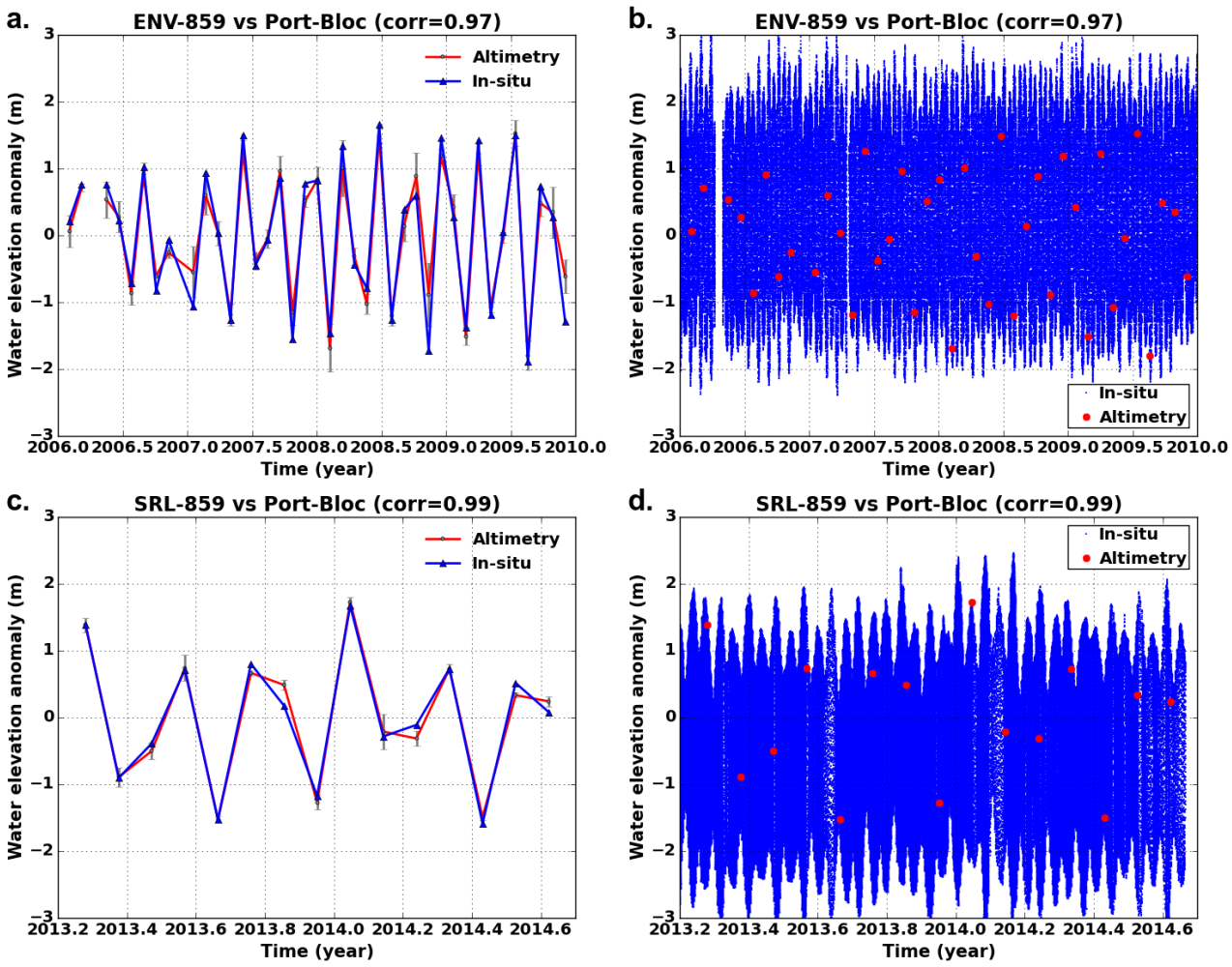


Figure 6. Comparison between virtual station 859 water elevation anomaly (red line on panels a. and c. and red dots on panels b. and d.), water elevation anomaly register by the Port-Bloc tide gage (blue line on panels a. and c.) at altimeter measurement times and all tide gage measurements (blue dots on panels b. and d.) for ENVISAT between 2006 and 2010 (panels a. and b.) and for Saral between 2013 and 2014 (panels c. and d.)

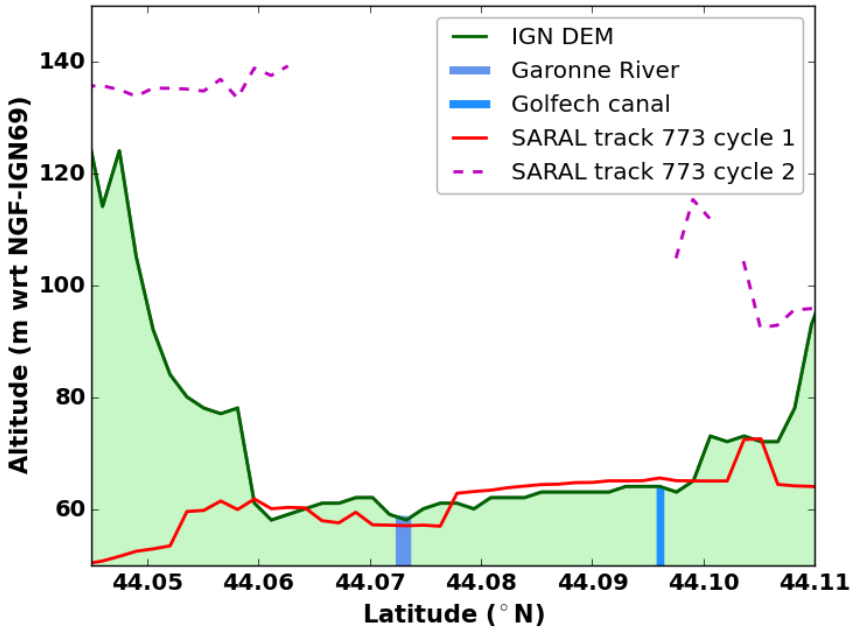


Figure 7. Comparison between IGN DEM (green line) along the SARAL 773 track (see Figure 1) over the Garonne River (its position is shown by the large blue polygon near 44.07°N, its elevation corresponds to the DEM and not to the actual river water level) and the artificial canal (tight light blue polygon near 44.09°N), elevations measured by SARAL/AltiKa for cycle 1 (10 April 2013, red curve) and for cycle 2 (15 May 2013, dashed magenta curve)

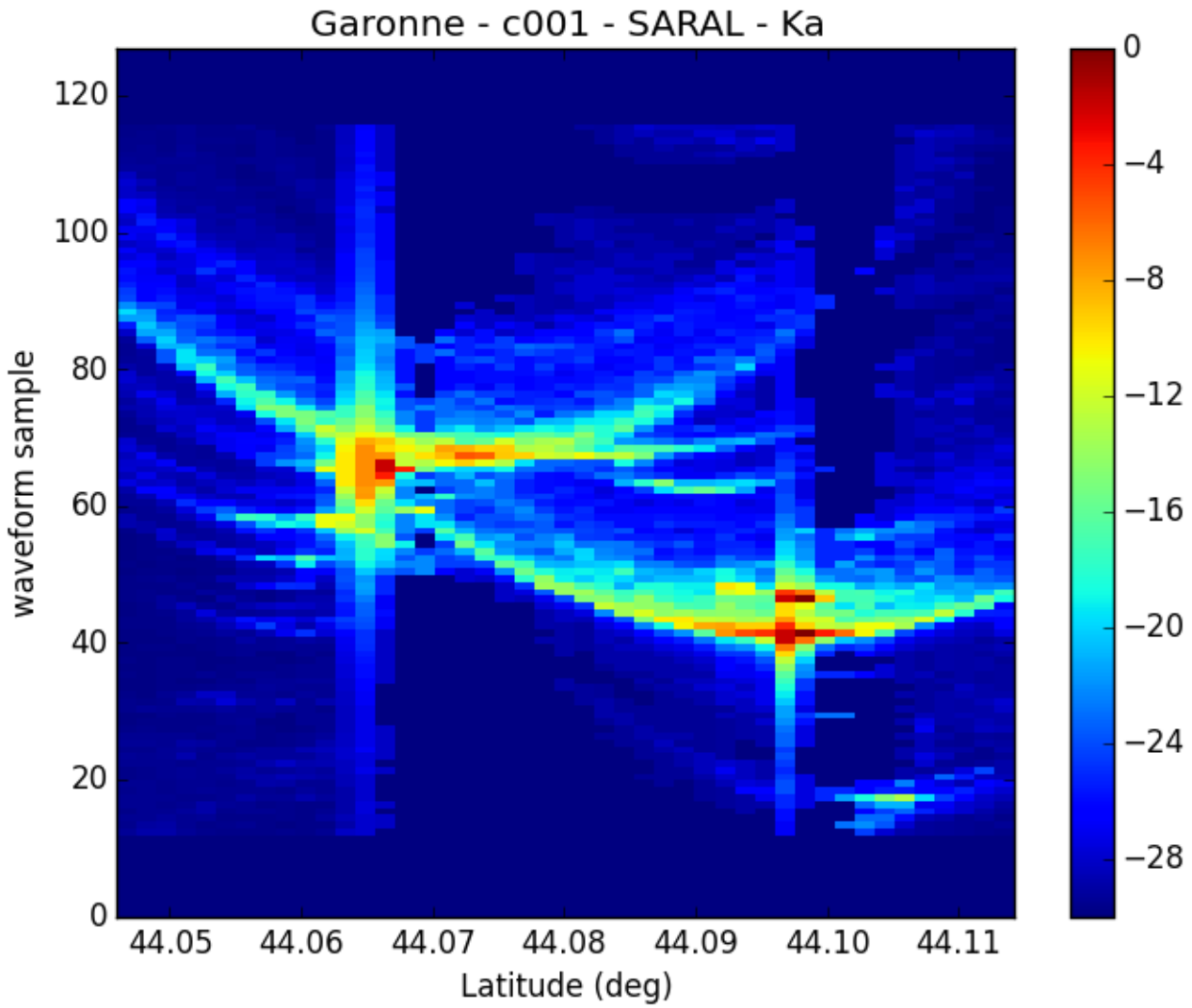


Figure 8. Radargram for SARAL/AltiKa cycle 1 pass over virtual station SRL-773.This is a representation of the successive waveforms measured on this pass. Each column represents one waveform (y-axis correspond to range gates number). Colors represent returned power received in each bin. A logarithmic scale (decibels) is used in order to be able to represent the large dynamic of received power.